Transition Metal Complexes of Heptadentate Bipyridine-Based Ligands

Alka Rani

A thesis submitted to

Auckland University of Technology

in fulfilment of the requirements for the degree of

Master of Philosophy

2026

Department of Chemistry

Abstract

This thesis investigates the coordination behaviour of first-row transition metal ions with novel heptadentate bipyridine-based ligands, focusing on the synthesis, characterization, and complexation properties of two new ligands N-([2,2'-bipydridin]-6-ylmethyl-N'-(2-(([2,2'-bipyridine]-6-ylmethyl)amino)ethyl)ethane-1,2-diamine (bmdet) and N-([2,2'-bipydridin]-6-ylmethyl-N'-(3-(([2,2'-bipyridine]-6-ylmethyl)amino)propyl)propane-1,3-diamine (bmdpt).

The ligands were synthesized via reductive amination of 2,2'-bipyridine-6-carbaldehyde with diethylenetriamine (bmdet) and dipropylenetriamine (bmdpt) respectively, and characterized by NMR spectroscopy and high-resolution mass spectrometry, confirming their structures and purity. Cobalt(III) complexes of these ligands were prepared using $Na_3[Co(CO_3)_3].3H_2O$ as the precursor. The X-ray crystal structure of $[Co_2(Hbmdet)_2Cl_2](ClO_4)_6$ confirmed the dimeric nature of this species, with two six-coordinate Co(III) centres bridged by the heptadentate ligands, with one donor atom of the ligand remaining unbound and protonated. Two chloride ions are bound within cavities formed by the aliphatic and bipyridine parts of the heptadentate ligands.

Mass spectrometric studies of complexes of bmdet and bmdpt with Cu^{2+}, Mn^{2+}, Fe^{2+}, Co^{2+}, Ni^{2+}, and Zn^{2+} demonstrated predominantly mononuclear species in solution. These analyses revealed peaks consistent with 1:1 metal-to-ligand complexes, often showing doubly charged ions corresponding to $[M(bmdet)]^{2+}$ or $[M(bmdpt)]^{2+}$ species. Notably, the mass spectra also indicated the presence of ligand-related species, including partially reduced or alternative ligand forms (e.g., L1), which influenced the observed complex distributions. For some metals, such as Mn and Cu, additional peaks suggested equilibrium mixtures involving free ligand, protonated ligand, and metal complexes with varying stoichiometries.

Job plot analyses for Cu^{2+} and Co^{2+} with both ligands in acetonitrile revealed differing predominant stoichiometries: Cu^{2+} complexes exhibited a metal-to-ligand ratio near 2:3, implying possible multinuclear or helical assemblies, whereas Co^{2+} complexes favored a 1:1 stoichiometry consistent with mononuclear species.

Overall, the combined crystallographic and mass spectrometric data indicate that while heptadentate ligands like bmdet and bmdpt are capable of forming stable complexes with first-row

transition metals, complete coordination of all seven donor atoms to a single metal centre is generally precluded. Instead, coordination involves six donor atoms, with the seventh often uncoordinated or facilitating the formation of multinuclear assemblies. These findings provide new insights into the design and binding modes of high-denticity ligands with first-row transition metals, expanding the understanding of coordination chemistry at the upper limits of ligand denticity and highlighting the complex equilibria present in solution.

Attestation of Authorship

I hereby declare that this submission is my own work and that, to the best of my knowledge and belief, it contains no material previously published or written by another person (except where explicitly defined in the acknowledgements), nor used artificial intelligence tools or generative artificial intelligence tools (unless it is clearly stated, and referenced, along with the purpose of use), nor material which to a substantial extent has been submitted for the award of any other degree or diploma of a university or other institution of higher learning.

	March 2nd, 2026
Signature	Date

Acknowledgements

First and foremost, I would like to express my deepest and most sincere gratitude to my supervisor, Professor Allan Blackman. Without his constant guidance, patience, and encouragement, this thesis would not have been possible. I truly could not have asked for a better supervisor. He supported me at every stage of my research journey, from teaching me fundamental concepts in chemistry to guiding me through more complex scientific challenges. He was always the first person I approached whenever I faced difficulties in the laboratory, whether it was running columns, interpreting data, or troubleshooting experiments. His mentorship has not only strengthened my research skills but also shaped my confidence as a scientist.

I would also like to extend my sincere thanks to my co-supervisor, Dr Emma Davison, for her valuable assistance and insightful discussions. Her guidance in analysing NMR spectra and helping resolve challenges with column chromatography was greatly appreciated. Her support contributed significantly to the successful completion of this work.

I am also grateful to our laboratory technicians, Iana and Adrian, for their continuous support with chemicals and laboratory resources. I would especially like to thank Adrian for his help in troubleshooting issues with the NMR instrument. My sincere thanks also go to Tony for promptly and efficiently running numerous mass-spectrometry samples.

I would like to acknowledge all my lab mates who made this one-year journey enjoyable and memorable. Their encouragement, discussions, and friendship created a positive and motivating research environment.

Finally, I owe my deepest gratitude to my family for their unconditional love and emotional support throughout this journey. A very special thanks to my husband, who always stood beside me, encouraging and supporting me at every step. Words are not enough to express my love and appreciation for my wonderful family.

Table of Contents

Abbreviations

δ	Chemical shift
AR	Analytical reagent
bipy	bipyridine
bmet	N,N'-bis(2,2'-bipyridin-6-ylmethyl)ethane-1,2-diamine
bmpp	N,N'-bis(2,2'-bipyridin-6-ylmethyl)propane-1,3-diamine
bmhx	N,N'-bis(2,2'-bipyridin-6-ylmethyl)hexane-1,6-diamine
bmbu	N,N'-bis(2,2'-bipyridin-6-ylmethyl)butane-1,4-diamine
bmpt	N,N'-bis(2,2'-bipyridin-6-ylmethyl)pentane-1,5-diamine
bmot	N,N'-bis(2,2'-bipyridin-6-ylmethyl)octane-1,8-diamine
bmdet	N-([2,2'-bipydridin]-6-ylmethyl-N'-(2-(([2,2'-bipyridine]-6-ylmethyl)amino)ethyl)ethane-1,2-diamine
bmdpt	N-([2,2'-bipydridin]-6-ylmethyl-N'-(3-(([2,2'-bipyridine]-6-ylmethyl)amino)propyl)propane-1,3-diamine
COSY	Correlations spectroscopy
^{13}C NMR	Carbon Nuclear Magnetic Resonance
dien	diethylenetriamine
DMSO	Dimethyl sulfoxide
en	ethylenediamine
ESI-MS	Electrospray Ionisation
^{1}H NMR	Proton Nuclear Magnetic Resonance
HRMS	High-Resolution Electrospray Ionization Mass Spectrometry
HSQC	Heteronuclear single quantum coherence
HMBC	Heteronuclear Multiple Bond Correlation
K	Equilibrium constant
LR	Laboratory reagent
LRMS	Low-Resolution Electrospray Ionization Mass Spectrometry

mer	meridional
m/z	Mass to charge ratio
TLC	Thin-layer chromatography
trien	triethylenetetramine
UV/vis	Ultraviolet-Visible

1. Introduction

1.1 Coordination Chemistry:

Coordination chemistry as a distinct area of chemistry began with the work of both Jørgensen and Werner in the late 19th/early 20th centuries. Since the formulation of Werner's coordination theory, the field has undergone continuous evolution, and now encompasses advanced theoretical models and technologically relevant applications.[1] Today, coordination chemistry underpins advances in homogeneous catalysis, molecular electronics, photochemistry, supramolecular chemistry, bioinorganic systems, and metal-based therapeutics. At its simplest, coordination chemistry involves the interaction of a transition metal with one or more ligands. Transition metals have partially filled d orbitals, which allow for variable oxidation states and different modes of bonding, while their range of different sizes allows for diverse coordination numbers.[2] On the other hand, ligands have a range of denticities, geometries, charges, and donor atom types, all of which lead to unique chemical and physical characteristics of the resulting metal complexes.

Multidentate ligands have long been a subject of interest in coordination chemistry.[3] Such ligands offer the possibilities of enhanced stability and greater structural control in the synthesis of coordination complexes. However, they also raise fundamental questions regarding the limits of metal coordination, especially when ligand denticity approaches or exceeds the typical coordination number of the metal ion. Addressing these questions is essential for advancing both theoretical understanding and practical ligand design strategies.

1.2 First-Row Transition Metals

The first-row transition metals (3d series) occupy a distinctive position in coordination chemistry due to their relatively small ionic radii, moderate ligand field strengths, and, with the exceptions of Co(III) and, to a lesser extent, Cr(III), rapid ligand exchange kinetics.[4] The first row transition metals often exhibit coordination behaviour that is more flexible than that of their second- and third-row counterparts.[5] One defining feature of first-row transition metals is their coordination number. This is the number of ligand donor atoms directly bonded to the metal ion. In first-row transition metals, the most common coordination numbers is six, and this is usually associated with an octahedral geometry. This geometry provides optimal orbital overlap and ligand field stabilization for many d-electron configurations.[6] Five-coordinate complexes, which display either

trigonal bipyramidal or square pyramidal geometries, are also commonly observed and often exhibit dynamic behaviour in solution. Four-coordinate complexes may be tetrahedral or square planar, depending on electronic configuration and ligand type.[7] The small sizes of the first row transition metal ions means that accommodation of seven or more donor atoms around a single metal ion is rare, as this leads to significant steric crowding. Such high coordination numbers are usually only achieved through careful multidentate ligand design .[8]

1.3 Ligands

Ligands play an important role in shaping the structure and properties of coordination complexes. The predominant classical interaction between a ligand and a transition metal is of the Lewis acid/base type. The ligand acts as a Lewis base, donating electron density to the metal centre through one or more donor atoms in a σ fashion, thus forming coordinate (or dative) covalent bonds. Depending on the donor atom, the ligand can also act as either a π-Lewis acid or π-Lewis base, accepting or donating π electron density from or to the metal ion. Such interactions are often found in ligands containing aromatic donors.[9] While any atom possessing a lone pair of electrons can potentially coordinate to a transition metal ion, ligands containing nitrogen-donor atoms are probably the most extensively studied in coordination chemistry due to their versatile bonding characteristics, tunable basicity, and compatibility with a wide range of metal ions.[10]

1.3.1 Denticity of Ligands:

Ligands in so-called 'classical' coordination complexes require at least one donor atom having a lone pair of electrons that can be donated to a transition metal to form a coordinate or dative bond. The denticity of a ligand refers to the number of donor atoms that a ligand uses to bind to a transition metal. Ligands such as water (H_2O) and ammonia (NH_3) only have a single atom bearing a lone pair, and as a result, can only use one atom to bind to a transition metal. Such ligands are called monodentate. The ethane-1,2-diamine ligand (figure 1), commonly known as ethylenediamine (a non-IUPAC name) and abbreviated en, is an example of a ligand that generally binds in a bidentate fashion, with both N atoms forming bonds to a single transition metal ion.

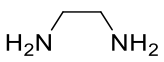

figure 1: The structure of the ethylenediamine (en) ligand.

It should be noted, however, that en can bind in a monodentate fashion using only one of the two N atoms, and although this is extremely rare, [11–15] it is thus technically incorrect to say that en is a bidentate ligand. In addition, en can act as a bridging ligand between two transition metal ions, and in this case, acts as a bis-monodentate ligand.[16] As the number of donor atoms in a ligand increases, so generally does the denticity of the ligand. Thus *N*-(2-aminoethyl)ethane-1,2-diamine (commonly called diethylenetriamine, or dien, figure 2) can bind in a tridentate fashion through all three N atoms,

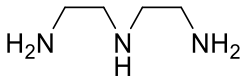

figure 2: The structure of the diethylenetriamine (dien) ligand

while N,N'-(ethane-1,2-diyl)di(ethance-1,2-diamine) (triethylenetetramine, trien, figure 3) can utilise all four N atoms to bind to a single transition metal ion in a tetradentate fashion. Ligands having more that one potential donor atom are generally termed polydentate or multidentate.

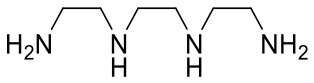

figure 3: The structure of the triethylenetetramine (trien) ligand

As noted above for the en ligand, it is possible for a multidentate ligand to bind to a single transition metal ion using less than the maximum number of donor atoms. Such binding is termed hypodentate, and may arise from careful choice of reaction conditions, or steric factors of the ligand. Thus, hypodentate complexes of both dien[17–20] and trien[21] have been reported.

1.3.2 Chelate rings:

When a ligand coordinates to a single transition metald ion using at least two donor atoms, a chelate ring is formed. The size of the chelate ring is determined by the number of atoms that separate the donor atoms in the ligand. For example, when an en ligand binds in a bidentate fashion, a 5-membered chelate ring is formed, containing the metal ion, the two donor N atoms, and the two C atoms of the ligand (figure 4).

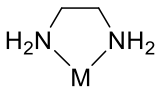

figure 4: A 5-membered chelate ring formed on coordination of en to a metal ion.

As the ligand is aliphatic, the resulting chelate ring is non-planar. Because of the requirement to accommodate a 90° (or at least close to 90°) bond angle about the metal ion, 5-membered chelate rings are generally most stable as they have the least ring strain. 4- and 6-membered chelate rings are also relatively common, but 7-membered and above are quite rare.

1.3.3 The chelate effect:

The stability of a transition metal complex can be determined by measurement of the equilibrium constant for its formation from the transition metal and the ligand(s). The equilibrium constant expression for the equilibrium

$$M(aq) + nL(aq) \rightleftharpoons ML_n(aq)$$

is

$$K = \frac{[ML_n]}{[M][L]^n}$$

and the value of K gives a measure of the stability of the complex – if K is large, the equilibrium lies to the right and the complex is formed in large amounts, and vice versa.

Numerous studies have shown that complexes formed from multidentate ligands, which contain chelate rings, generally exhibit significantly larger values of K than do complexes containing only monodentate ligands. This has been termed The Chelate Effect.[8] For example, consider the chemically similar complex cations $[Ni(NH_3)_6]^{2+}$ and $[Ni(en)_3]^{2+}$. Both have a Ni^{2+} ion coordinated to 6 ligand N atoms, and display similar octahedral geometries. The equilibria for the formation of these complexes are given below.

$Ni^{2+}(aq) + 6NH_3(aq) \rightleftharpoons [Ni(NH_3)_6]^{2+}(aq)$ $\quad\quad$ $\log K = 8.61$

$Ni^{2+}(aq) + 3en(aq) \rightleftharpoons [Ni(en)_3]^{2+}(aq)$ $\quad\quad$ $\log K = 18.28$

Firstly, it should be noted that the equilibrium constants for the formation of both complexes are massive, and that both equilibria lie very much towards products. However, it is obvious that the en complex is some 10 orders of magnitude more thermodynamically stable than the NH_3 complex. This must therefore mean that the value of ΔG^o for the formation of the en complex is significantly more negative than that for the NH_3 complex. This can be explained in terms of the following equations.

$$\Delta G^\circ = -RT \ln K$$

$$\Delta G^\circ = \Delta H^\circ - T\Delta S^\circ$$

As can be seen, there are both enthalpic and entropic contributions to the value of ΔG^o. Schwarzenbach, in 1952, showed that coordination of a multidentate ligand to a metal ion resulted in a larger increase in entropy than the corresponding reaction with a monodentate ligand. This is because coordination of a multidentate ligand releases 6 aqua ligands from a hydrated metal ion but binds three or fewer ligands to the metal in the process; the same reaction with a monodentate ligand would consume 6 monodentate ligands while the 6 aqua ligands are released, giving essentially no increase in entropy. As can be seen in the equation above, a larger positive value of ΔS^o favours a larger negative value of ΔG^o in situations where the values of ΔH^o are comparable.

The enthalpic effects in these types of reactions are usually negligible, as has been shown from the small values of enthalpy changes for reactions of the type

$$[M(NH_3)_6]^{n+} + 3en \rightleftharpoons [M(en)_3]^{n+} + 6NH_3$$

One important factor in these reactions is that the polar N atoms in ethylenediamine are bound together in relatively close proximity and therefore some of their mutual repulsions are overcome before complexation, whereas in ammonia the individual molecules are separated, meaning that formation of the monodentate complex will involve a larger energy barrier.

The size of the chelate ring formed in these reactions must also be considered. Initial coordination of the chelating ligand to a metal ion will give a transient monodentate complex, and coordination of a second donor atom to the same metal ion will be easier for small chain lengths between the donor atoms. This is because the second donor atom is constrained to be in the vicinity of the metal

ion when the chain length, and hence chelate ring size, is small, thus increasing its probability of coordination relative to a ligand having a long distance between its donor atoms.

It is well known that 5- and 6-membered rings are the most thermodynamically stable chelate rings in chemistry. Molecular mechanics calculations on 5- and 6-membered chelate rings give the optimum bond lengths and angles shown in figure 1.3. For 6-membered rings, the N-M-N bite angle is larger, and the M-N bond lengths and distances between the two N atoms is smaller than those in 5-membered chelate rings. This therefore suggests that the 6-membered ring will be preferred for small metal ions such as Cu(II) and Ni(II), while for larger metal ions , the presence of a 5-membered ring would give complexes of lower energy.

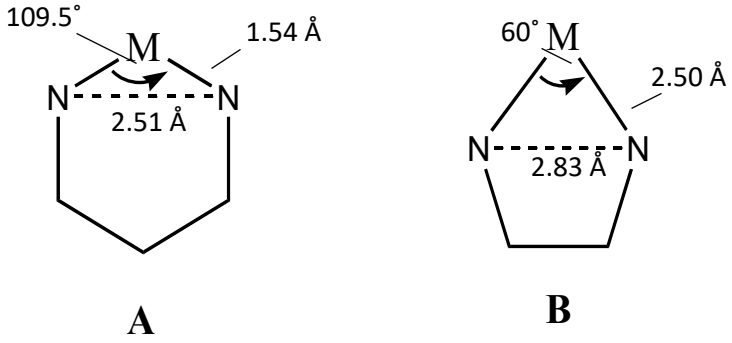

figure 5: The optimised geometries for (A) a 6-membered chelate ring, and (B) a 5-membered chelate ring in a metal complex.[22]

The net result is that multidentate ligands which form 5- and/or 6-membered chelate rings on coordination to a metal ion would be expected to show significant stability when compared to lower-dentate congeners, and, from a purely thermodynamic standpoint, all available donor atoms in the multidentate ligand would be expected to bind to the metal ion. However, this may not always be the case if the ligand, or the metal-ligand complex, has unfavourable steric factors.

1.4 Amine ligands

Amine ligands occupy a seminal place in coordination chemistry. Transition metal complexes of the simplest amine ligand, ammonia, NH_3, formed much of the basis of the early work by Jørgensen and Werner, and these complexes were crucial in the development of concepts such as coordination number and oxidation state that underpin modern coordination chemistry. Similarly,

complexes containing the en ligand were originally studied in order to understand concepts such as geometric and optical isomerism in coordination complexes.

1.4.1 Aliphatic amine ligands.

A large amount of work has been carried out on transition metal complexes of aliphatic polyamine ligands. Of particular interest has been the series of polyamine ligands based on en. These ligands contain two (en), three (dien), four (trien), five (tetraen), and six (pentaen) nitrogen donor atoms, and form exclusively 5-membered chelate rings on coordination to a transition metal ion. The ligands are very flexible and can bind in many different ways to a transition metal ion, as they are relatively unconstrained. As the denticity of the ligand increases, so does the number of possible isomers, owing to the different possible foldings of the ligand, the different possible conformations of the chelate rings, and the different possible relative configurations of the secondary N-H protons. Indeed, 7 isomers of the $[Co(pentaen)]^{3+}$ complex have been prepared and characterised, two of which are shown in figure 6.

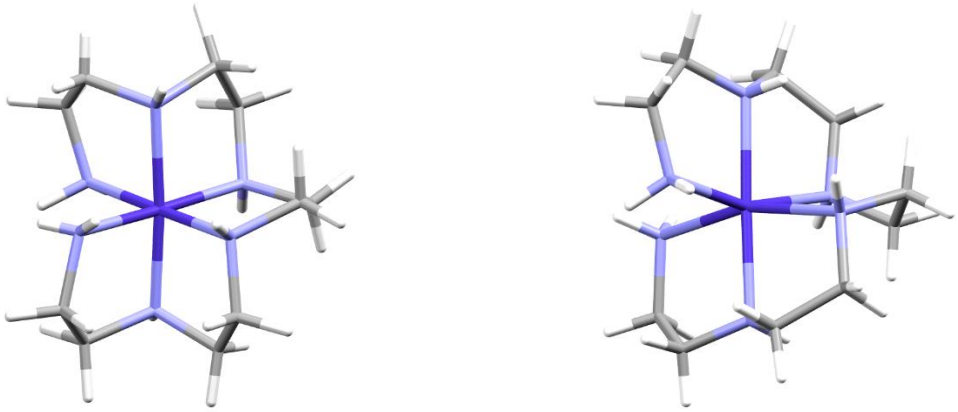

figure 6: Two isomers of the $[Co(pentaen)]^{3+}$ ion. Left: the *ffff* isomer.[23] Right: the *mffm* isomer.[24]

The large number of possible isomers can be a hinderance in the characterisation of such complexes, with extensive chromatographic separations often being required before crystallisation can be successful.

1.4.2 Aromatic amine ligands

A large number of monodentate and multidentate amine ligands containing aromatic N donor atoms are known. The majority of these are based on the pyridine molecule, a 6-membered heterocyclic ring containing a single N donor atom, and many complexes containing this

monodentate ligand, and its substituted derivatives, are known. Of importance to this thesis, and to coordination chemistry in general, is the 2,2'-bipyridine ligand (figure 7).[25]

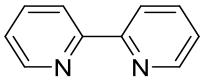

figure 7: The structure of 2,2′-bipyridine

This was first prepared by Blau in 1888, from the dry distillation of Cu(II) pyridine-2-carboxylate, and since this time thousands of complexes containing 2,2'-bipyridine have been prepared and characterised. The free ligand preferentially adopts a conformation in which the two N atoms are mutually *trans* to each other,[26] but in metal complexes, both N atoms bind to a single metal ion in a *cis* conformation to give a 5-membered chelate ring. Owing to the sp^2 hybridisation of all atoms in the 2,2'-bipyridine ligand, the chelate ring is essentially planar, in contrast to the conformational possibilities found in 5-membered aliphatic chelate rings, and this reduces the number of possible isomers that can be formed. The ligand has a bite angle around 78–82°, which is the range that fits well with the coordination preferences of many first-row transition metals. It behaves electronically as a strong σ-donor, and a moderate π-acceptor, and as a result its metal complexes generally display high thermodynamic stability.[27]

The bipyridine unit is relatively rigid, in that only rotation about the interannular bond is permitted. As a result, polypyridine ligands analogous to the multidentate aliphatic amine ligands discussed above have little conformational freedom, and indeed, the 2,2′:6′,2″:6″,2‴:6‴,2⁗:6⁗,2⁗′-sexipyridine ligand (figure 8) cannot bind all 6 N atoms to a single metal ion, and instead forms double helical complexes containing two or three metal ions. [28,29]

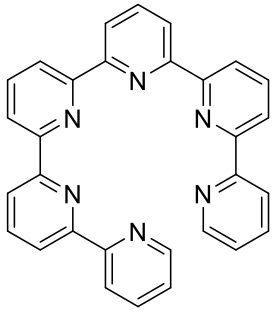

figure 8: The 2,2′:6′,2″:6″,2‴:6‴,2⁗:6⁗,2⁗′-sexipyridine ligand

1.4.3 Aliphatic-aromatic amine ligands.

Given the high thermodynamic stability of complexes containing bipyridine units, and the flexibility of multidentate amine ligands, it was obvious that the synthesis of multidentate ligands incorporating both features should be investigated. In 2007, the synthesis of the bmet (bmet = N,N'-bis(2,2'-bipyridin-6-ylmethyl)ethane-1,2-diamine) ligand (figure 9) was reported. [30]

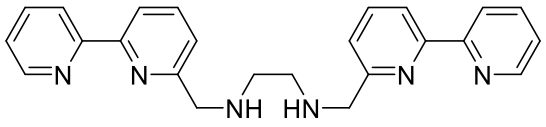

figure 9: Structure of the bmet ligand

This was prepared by the reductive amination of ethylenediamine with 2,2'-bipyridine-6-carboxaldehyde, using $NaBH_4$ as the reductant. The bmet ligand is a hexadentate ligand incorporating both aromatic and aliphatic N donor atoms, thus forming thermodynamically stable complexes that have some ligand flexibility. Unlike the 2,2′:6′,2″:6″,2‴:6‴,2⁗:6⁗,2⁗′-sexipyridine ligand discussed above, bmet can bind all 6 donor atoms to a single transition metal ion. This was demonstrated in the crystal structure of the complex $[Co(bmet)](ClO_4)_3.H_2O$, the complex being prepared from reaction of the ligand hydrochloride salt with $Na_3[Co(O_2CO)_6].3H_2O$ in aqueous solution. This also showed that the ligand, while flexible, could only bind in a single configuration to the metal ion, such that the bipy N atoms and the neighbouring aliphatic N atom lie mutually *mer*, figure 10

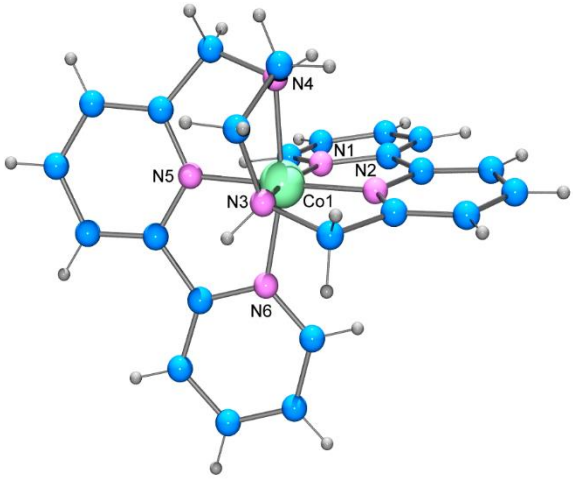

figure 10: X-ray Crystal structure of the $[Co(bmet)]^{3+}$ cation.

This lack of configurational flexibility thereby simplifies characterisation. ^{1}H NMR was consistent with the observed rigidity of the ligand in the complex; the observed geminal coupling of the methylene protons showed that the 5-membered chelate rings associated with these were static. The UV/vis spectrum of the complex was consistent with bmet being an extremely strong-field ligand, and this could be explained by the presence of two particularly short Co-N bonds (1.8653(19) Å and 1.8636(19) Å). In addition, to bmet, the syntheses and characterisation of two other similar ligands, N,N'-bis(2,2'-bipyridin-6-ylmethyl)propane-1,3-diamine (bmpp) and N,N'-bis(2,2'-bipyridin-6-ylmethyl)hexane-1,6-diamine (bmhx), were also reported. These, along with other new ligands N,N'-bis(2,2'-bipyridin-6-ylmethyl)butane-1,4-diamine (bmbu), N,N'-bis(2,2'-bipyridin-6-ylmethyl)pentane-1,5-diamine (bmpt), and N,N'-bis(2,2'-bipyridin-6-ylmethyl)octane-1,8-diamine (bmot) were studied in a subsequent paper. [31]

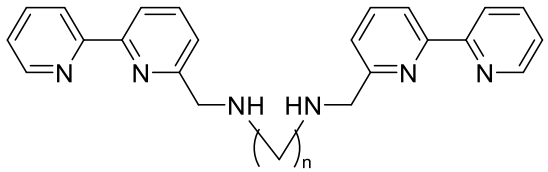

figure 11: Structures of the bmet (n = 2), bmpp (n = 3), bmbu (n = 4), bmpt (n = 5), bmhx (n = 6), and bmot (n = 8) ligands.

These were prepared by reductive amination reactions analogous to that used for the synthesis of bmet, and X-ray crystal structures of $[Mn(bmet)](ClO_4)_2$, $[Ni(bmet)](ClO_4)_2$, $[Fe(bmet)](ClO_4)_2$, $[Mn(bmpp)](ClO_4)_2.2MeCN$, and $[Co(bmpp)](ClO_4)_3.H_2O$ were reported. The crystal structures of $[Cu(bmet)](ClO_4)_2.H_2O$, $[Cu(bmet)]Br_2.2MeCN$, and $[Zn(bmet)](ClO_4)_2.H_2O$ were also reported in a subsequent paper,[32] but no crystalline complexes of the bmbu, bmpt, bmhx and bmot ligands could be obtained. It was found that only mononuclear complexes were formed for the bmet, bmpp and bmbu ligands. However, electrospray ionization mass spectrometry (ESI-MS), provided strong evidence for the formation of multinuclear complexes with the bmpt and bmot ligands. The mass spectra showed mono-, di-, and trinuclear species, with dinuclear complexes being the most common. For example, the observed ESI-MS spectrum of an equimolar solution of $Ni(ClO_4)_2.6H_2O$ and bmpt in acetonitrile is a composite of the calculated spectra of mononuclear $[Ni(bmpt)]ClO_4^+$, binuclear $[Ni_2(bmpt)_2](ClO_4)_2^{2+}$, and trinuclear $[Ni_3(bmpt)_3](ClO_4)_3^{3+}$. (figure 12). Fe(II) and Mn(II) complexes of the bmot ligand showed similar patterns. These findings

indicate that the solution contains a mixture of species in equilibrium, and that longer alkyl chains on the ligand increase the tendency to form multinuclear assemblies.

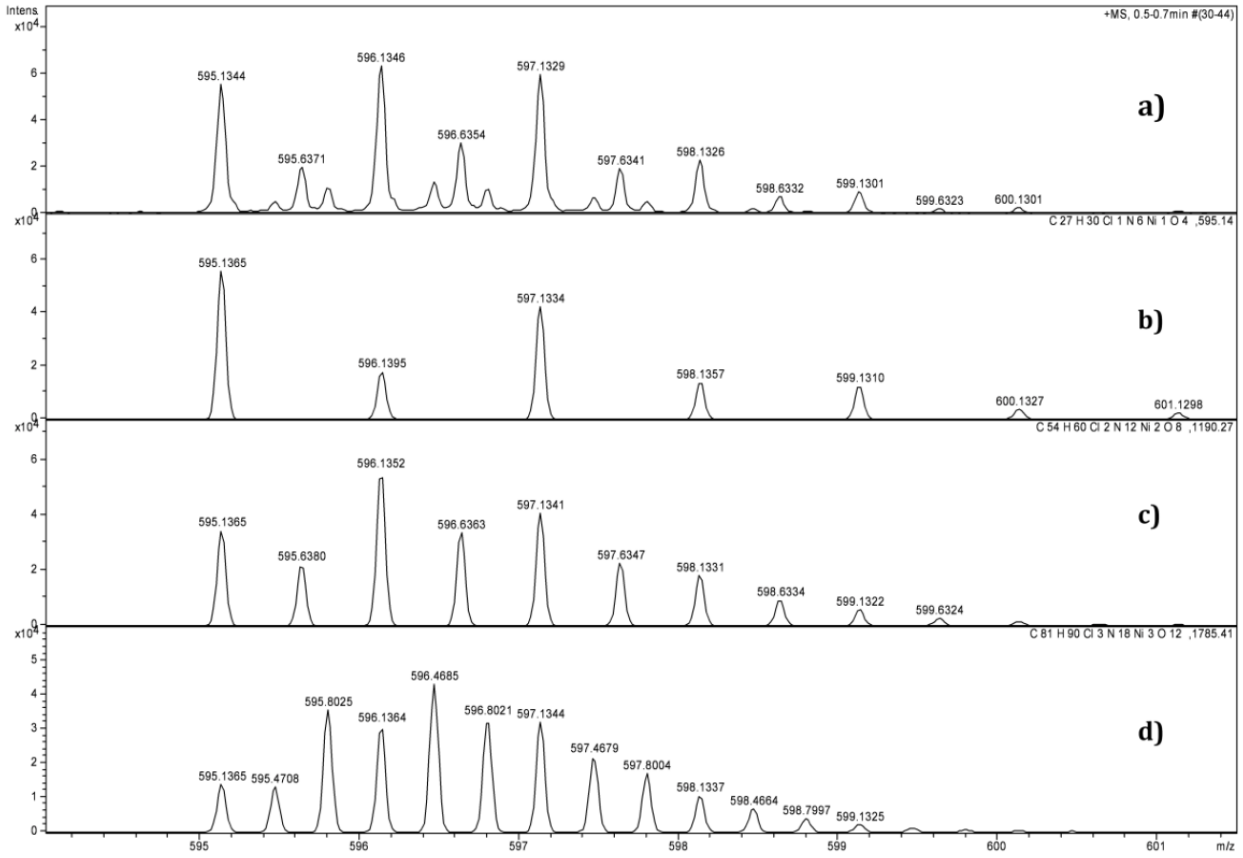

figure 12: (a) Experimental ESI-MS of an equimolar solution of $Ni(ClO_4)_2.6H_2O$ and bmpt in acetonitrile. (b) Calculated ESI-MS of $[Ni(bmpt)]ClO_4^+$. (c) Calculated ESI-MS of $[Ni_2(bmpt)_2](ClO_4)_2^{2+}$. (d) Calculated ESI-MS of $[Ni_3(bmpt)_3](ClO_4)_3^{3+}$.

This is presumably because of the increasing size of the central chelate ring as the alkyl chain gets longer – in the case of the octane ligand, an 11-membered central chelate ring would be formed, for example. The strain present in such large chelate rings is significant and often precludes their formation, and this would then encourage formation of multinuclear species. While crystals of the di- and trinuclear complexes could not be obtained, it was assumed that these would be helical in nature, by analogy with the sexipyridine complexes discussed above. Interestingly, the very similar series of imine ligands shown in figure 13 were found to form only dimeric, trimeric and tetrameric Ag^+ complexes, presumably owing to the lack of flexibility imparted by the C=N unit not allowing formation of a mononuclear complex. The ligands themselves were not isolated.[33]

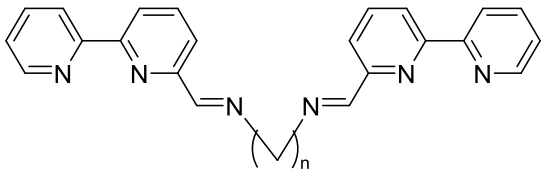

figure 13: Structures of the imine ligands (n = 0, 2, 3, 4).

1.5 Heptadentate N-donor ligands.

As stated above, it is very rare that first row transition metal ions can accommodate 7 donor atoms in a mononuclear complex. Therefore, it is of interest to see what will occur when a heptadentate ligand binds to a first row transition metal ion.

The simplest heptadentate aliphatic nitrogen donor ligand is hexaen (figure 14).

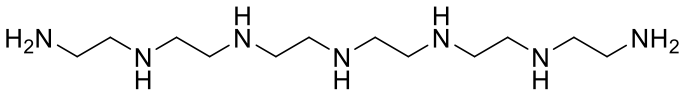

figure 14: The structure of the hexaen ligand.

However, quite remarkably, it appears that no transition metal complexes of this ligand have been structurally characterised, or even reported. A Scifinder search of this ligand gives 508 hits, 501 of which are patents; none of the remaining 7 journal articles, which date back to only 2006, mention transition metal complexes of this ligand. It is also surprising is that the heptadentate ligand 1, containing a central pyridine ring (figure 15), has not been reported, while there is only a single report of the heptadentate bis(pyridyl) ligand 1,15-bis(2-pyridyl)-2,5,8,11,14-pentaazapentadecane (pytetren) (figure 16). The latter reported protonation constants and formation constants for the ligand with some transition metals (Co^{2+}; log K_{ML} = 22.67: Ni^{2+}; log K_{ML} = 26.25: Cu^{2+}; log K_{ML} = 28.46: Zn^{2+}; log K_{ML} = 19.90), but did not determine the nature of the ligand binding.[34]

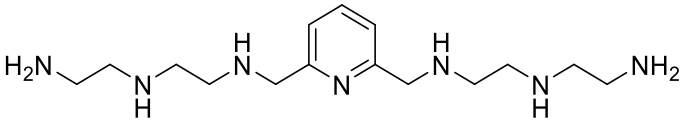

figure 15: The structure of ligand 1

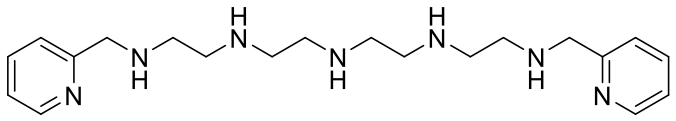

figure 16: The structure of ligand 1,15-bis(2-pyridyl)-2,5,8,11,14-pentaazapentadecane (pytetren).

A search of the Cambridge Structural Database shows that, surprisingly, there is only one example of a mononuclear complex of a linear heptadentate ligand containing mixed amine and imine donors (figure 17),[35]

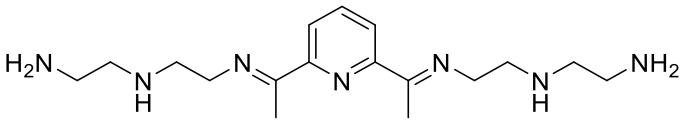

figure 17: The structure of a heptadentate ligand containing amine and imine donors

and no mononuclear complexes of any linear heptadentate amine ligand have been reported. With this in mind, the main goal of this study is to determine the binding behaviour of first-row transition metals with heptadentate bipyridine-based ligands. Can mononuclear coordination of such ligands occur so that all ligand donor atoms are bound to the metal ion? And if not, what is the resulting binding behaviour? Does the metal ion bind 6 of the 7 donors to give an octahedral complex? Or are multinuclear complexes formed in which 6-coordination can be achieved at each metal ion?

2. Experimental

2.1 Instrumentation

All NMR spectra were recorded using a Bruker Ascend 400 NMR spectrometer operating at 400 MHz for ^{1}H nuclei and 101 MHz for ^{13}C nuclei. Samples were dissolved (500 µL) in either deuterated chloroform ($CDCl_3$) or deuterated water (D_2O). The residual solvent peaks specific to the deuterated solvents were used as internal references: $CDCl_3$: 7.26 ppm (^{1}H NMR) and 77.36 ppm (^{13}C NMR); D2O: 4.79 ppm (^{1}H NMR). All ^{1}H NMR spectra are reported as: chemical shift δ (ppm), multiplicity (s = singlet, d = doublet, t = triplet, q = quartet, and m = multiplet).

High-resolution mass spectrometry (HRMS) analysis was recorded on a Thermo Orbitrap Exploris 120, and Low-resolution mass spectrometry (LRMS) analysis was conducted on an Agilent 1260 Infinity Quaternary LC Systems instrument. Both used electrospray ionisation (ESI) in positive mode. Post-run analyses for HRMS were done using Freestyle 1.8 SP2 QF1 software. Samples for HRMS and LCMS were prepared in methanol (MeOH) or acetonitrile (CH_3CN) at a concentration of less than 1 mg/mL. HRMS and LCMS data reported as: molecular formula, calculated parent ion (m/z) and observed parent ion (m/z).

UV–Vis absorption spectra were measured using an Agilent Cary 60 spectrophotometer. Samples were dissolved in acetonitrile (CH_3CN) and methanol (MeOH) and analysed in quartz cuvettes with a 1 cm path length.

Thin-layer chromatography (TLC) analyses were carried out on aluminium-backed plates coated with Merck Silica Gel 60 F_{254} (0.25 mm) or Macherey–Nagel aluminium oxide N (0.2 mm) with a UV_{254} fluorescent indicator. Appropriate solvent systems were used for development, and spots were visualised under ultraviolet light at 254 nm. Column chromatography was performed using either silica gel 60 (Aldrich) or basic activated aluminium oxide as the stationary phase, with suitable eluents selected for separation.

All chemicals used were of laboratory reagent (LR) or analytical reagent (AR) grade and utilised as provided. Syntheses were conducted under aerobic conditions unless specified otherwise.

2.2 Ligand Preparation

2.2.1 6-methyl-2,2'-bipyridine

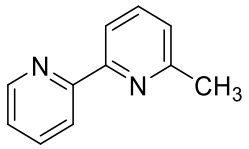

figure 18: The chemical structure of 6-methyl-2,2'-bipydridine.

Method A

This was synthesized using a modified method of Liao *et al.*[36]

A mixture of $NiCl_2 \cdot 6H_2O$ (1.21 g, 5.00×10^{-3} mol) in dimethylformamide (200 mL) in a 500 mL round-bottom flask was heated at 40°C, yielding a turquoise solution. To the above solution, 2-bromo-6-methylpyridine (1.14 mL, 10.0×10^{-3} mol), 2-bromopyridine (2.26 mL, 25.0×10^{-3} mol), anhydrous LiCl (4.41 g, 0.105 mol), and zinc dust (8.15 g, 0.126 mol) were added. Once the temperature reached 50°C, a few grains of iodine crystals and 10 drops of glacial acetic acid were added to initiate the reaction. A mixture of 2-bromo-6-methylpyridine (2.28 mL, 20.0×10^{-3} mol) and 2-bromopyridine (4.53 mL, 50.0×10^{-3} mol) in dimethylformamide (50 mL) was added dropwise to the reaction mixture at 60°C over a period of 3 hours. The reaction mixture was then stirred overnight at 60°C.

The reaction mixture (grey-black colour) was cooled to room temperature. With constant stirring, 1 M HCl(aq) (150 mL) was added slowly to consume the zinc dust, thereby forming a milky solution. The solution was made alkaline by adding aqueous ammonia solution (100 mL, 28 %), and the solution turned clear black. This was extracted with methylene chloride (3 × 100 mL). The combined organic layers were dried over Na_2CO_3, filtered, and reduced to low volume (rotavap). Toluene (50 mL) was added, and the solution was reduced to a low volume (rotavap, 60°C) to remove the remaining dimethylformamide; this was repeated three times. The product was purified by column chromatography on silica gel (60) and was initially eluted with chloroform, then with a chloroform/methanol (98:2) mixture, and finally with a chloroform/methanol (95:5) mixture. This purification method was attempted several times; however, the desired product was not obtained. Therefore, method B was employed for the synthesis of 6-methyl-2,2'-bipyridine.

Method B

Caution: MeLi is potentially pyrophoric when exposed to air.

This was synthesized using a modified method of Schmalzl and Summers.[37]

2,2'-bipyridine (18.42 g, 0.1180 mol) was dissolved in dry ethyl ether (225 mL) under N_2. To this stirred solution was added a solution of methyl lithium in dimethoxymethane (3.1 M, 100 mL, 0.31 mol) via cannula over a period of 10-15 minutes. The solution turned deep red instantly and was stirred continuously at room temperature under a N_2 atmosphere for 3 hours. This solution was then poured slowly onto 300 g of finely crushed ice with constant stirring, resulting in a bright yellow solution. This solution was then extracted with diethyl ether (3 × 150 mL), and the combined organic layers were dried over anhydrous Na_2SO_4, filtered, and the filtrates were reduced to dryness (rotavap) to yield dihydro-6-methyl-2,2'-bipyridine as a dark brown oil. This was then heated for 2 h at 90°C under vacuum to convert dihydro-6-methyl-2,2'-bipyridine to 6-methyl-2,2'-bipyridine. The crude product was purified by chromatography on an alumina column packed with a solvent mix of dichloromethane/toluene (50:50). The column was initially eluted with dichloromethane/toluene (50:50), then with dichloromethane (100%). The eluate was monitored by TLC, and the second band was found to contain the desired product. This was collected and reduced to dryness (rotavap), yielding a light-yellow oil (8.65 g , 43.08% based on 2,2'-bipyridine). ^{1}H NMR (400 MHz, $CDCl_3$): δ 8.57 (ddd, 1H, H-6'), 8.31 (dt,1H, H-5'), 8.07 (d, 1H, H-3), 7.79 – 7.62 (m, 1H, H-3'), 7.62 – 7.51 (m, 1H, H-4), 7.20 – 7.10 (m, 1H, H-4'), 7.05 (d, 1H, H-5), 2.53 (s, 3H, H-7); ^{13}C NMR (101 MHz, $CDCl_3$) δ 157.9 (C2), 156.5(C2'), 155.6(C6), 149.1(C6'), 137.1(C4), 136.8(C3'), 123.5(C4'), 123.3(C5), 121.2(C5'), 118.1(C3), 24.7(C7). HRESI-MS: Calculated (*m/z*) for $C_{11}H_{11}N_2^+$ $[M+H]^+$ (*m/z*) = 171.0920; found (*m/z*) = 171.0916

2.2.2 6,6'-dimethyl-2,2'-bipyridine

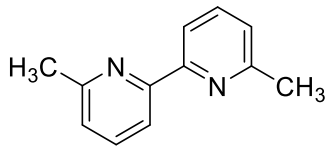

figure 19: The chemical structure of 6,6'-dimethyl-2,2'-bipydridine.

This was synthesized using a modified method of Liao *et al.*[36]

A mixture of $NiCl_2 \cdot 6H_2O$ (1.21 g, 5.21×10^{-3} mol) and dimethylformamide (200 mL) in a 500 mL round-bottom flask was heated at 40°C, yielding a turquoise solution. To the above solution, 2-

bromo-6-methylpyridine (1.14 mL, 0.0100 mol), anhydrous LiCl (4.43 g, 0.105 mol), and zinc dust (7.82 g, 0.120 mol) were added. Once the temperature reached 50°C, a few grains of iodine crystals and 10 drops of glacial acetic acid were added to initiate the reaction. 2-bromo-6-methylpyridine (10.24 mL, 9.000×10^{-2} mol) was added dropwise to the reaction mixture at 60°C over 3 hours. The reaction mixture was then stirred overnight at 60°C.

The reaction mixture (grey-black colour) was cooled to room temperature. With constant stirring, 1 M HCl(aq) (150 mL) was added slowly to consume the zinc dust, thereby forming a milky solution. The solution was made alkaline by adding aqueous ammonia solution (100 mL, 28 %), and it turned clear black. This was extracted with methylene chloride (3 × 100 mL). The combined organic layers were dried over Na_2CO_3, filtered, and reduced to low volume (rotavap). 50 mL of toluene was added, and the solution was reduced to a low volume (rotavap, 60°C) to remove the remaining dimethylformamide; this was repeated four times. The product obtained was a light orange crystalline solid (6.83g, 74.16% based on 2-bromo-6-methylpyridine). ^{1}H NMR (400 MHz, $CDCl_3$): δ 8.17 (d, J = 7.8, Hz, 2H), 7.68 (t, J = 7.7 Hz, 2H), 7.16 (t, J = 8.5 Hz, 2H), 2.63 (s, 6H); ^{13}C NMR (101 MHz, $CDCl_3$): δ 157.9, 156.0, 137.0, 123.0, 118.2, 24.7. LRESI-MS: Calculated (*m/z*) for $C_{12}H_{13}N_2^+$ $[M+H]^+$ (*m/z*) = 185.1070; found (*m/z*) = 185.1

2.2.3 2,2'-bipyridine-6-carbaldehyde

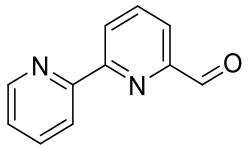

figure 20: The chemical structure of 2,2'-bipyridine-6-carbaldehyde.

This was synthesized using a modified method of Heirtzler *et al*.[38]

A mixture of 6-methyl-2,2'-bipyridine (11.73 g, 6.890×10^{-2} mol) and selenium dioxide (12.22 g, 1.101×10^{-1} mol) was refluxed in a solution of dioxane (325 mL) and deionised water (2.0 mL) under N_2 gas for 3 h to give a dark orange solution. The reaction mixture was then cooled to room temperature to give a cloudy mixture. To this was then added further deionised water (2.0 mL) and selenium dioxide (12.22 g), resulting in a slight colour change. Refluxing was then continued for a further 26 hours.

The reaction mixture was filtered through celite to remove metallic selenium, and the filter pad was washed with warm dioxane (50°C, 3 × 20 mL) and warm ethyl acetate (50°C, 3 × 20 mL), causing the filtrate to turn a milky cream colour. On cooling of the reaction mixture, an oily residue was formed, which was dissolved in methanol and reduced to dryness (rotavap) to give a dark yellow oil, which turned to a pale orange solid overnight.

The crude product was purified by column chromatography on silica gel (Silica gel 60). The crude product was dissolved in a small amount of dichloromethane, 7 g of silica gel was added, and the solid was dry-loaded on the column. Initial, elution with ethyl acetate/dichloromethane (15:85) and then with ethyl acetate/dichloromethane (50:50) removed the product. The product was obtained as a yellow oil on drying (rotavap), which solidified to a yellow powder over time (3.22 g, 25.37% based on 6-methyl-2,2'-bipyridine). ^{1}H NMR (400 MHz, $CDCl_3$): δ 10.18 (d, 1H), 8.72 (ddd, 1H), 8.69 – 8.62 (m, 1H), 8.56 (dt, 1H), 8.03 – 7.95 (m, 2H), 7.88 (td,1H), 7.37 (ddd, 1H).^{13}C NMR (101 MHz, $CDCl_3$) δ 194.1, 157.0, 155.3, 152.7, 149.7, 138.3, 137.5, 125.5, 124.7, 121.8, 121.6. HRESI-MS: Calculated (*m/z*) for $C_{11}H_9N_2O^+$ $[M+H]^+$ (*m/z*) = 185.0710; found (*m/z*) = 185.0709.

2.2.4 N-([2,2'-bipydridin]-6-ylmethyl-N'-(2-(([2,2'-bipyridine]-6-ylmethyl)amino)ethyl)ethane-1,2-diamine (bmdet)

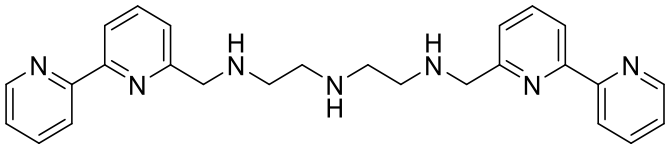

figure 21: The chemical structure of bmdet.

A solution of 2,2'-bipyridine-6-carbaldehyde (1.96 g, 1.06×10^{-2} mol) and diethylenetriamine (0.52 mL, 5.3×10^{-3} mol) in methanol (78 mL) was heated under reflux for 2 h with constant stirring. The reaction mixture was cooled to room temperature, and $NaBH_4$ (0.49 g, 1.3×10^{-2} mol) was added slowly, causing the solution to bubble. The mixture was stirred for a further 2 h, the resulting solution was filtered through celite, the filter pad was washed with methanol (30 mL), and the combined filtrates were reduced to dryness (rotavap), yielding a yellow residue. This was dissolved in deionised water (20 mL) and was extracted with chloroform (3 × 20 mL). The combined organic layers were dried over anhydrous Na_2SO_4, the mixture was filtered and the filtrate was reduced to dryness (rotavap). The product was obtained as a dark yellow oil (2.86 g,

61.51% based on 2,2'-bipyridine-6-carbaldehyde). ^{1}H NMR (400 MHz, $CDCl_3$) δ 8.67 (dq, 2H, H13), 8.43 (dt, 2H, H10), 8.26 (dd, 2H, H7), 7.78 (td, 2H,H12), 7.75 (t, 2H, H6), 7.27 (m, 6H, H5 /H11), 3.99 (s, 4H, H3), 2.83 (m, 8H, H1/H2); ^{13}C NMR (101 MHz, $CDCl_3$) δ 159.3(C8), 156.2(C9), 155.5(C4), 149.1(C13), 137.3 (C6), 136.8 (C12), 123.6 (C11), 122.2(C5), 121.1(C10), 119.2(C7), 55.1(C3), 49.6 and 49.2(C1/2). HRESI-MS: Calculated (*m/z*) for $C_{26}H_{30}N_7^+$ $[M+H]^+$ (*m/z*) = 440.2560, found (*m/z*) = 440.2556; calculated (*m/z*) for $C_{26}H_{31}N_7^{2+}$ $[M+2H]^{2+}$ (*m/z*) =220.6310, found (*m/z*) = 220.6215.

2.2.5 Preparation of bmdet.3HCl

1 g of bmdet was dissolved in 1 M HCl (50 mL) and reduced to dryness (rotavap) to give a pale-yellow solid. To this was dissolved in 20 mL of ethanol and reduced to dryness (rotavap). This was repeated three times, yielding bmdet.3HCl as a pale-yellow solid (1.42 g).

2.2.6 N-([2,2'-bipydridin]-6-ylmethyl-N'-(3-(([2,2'-bipyridine]-6-ylmethyl)amino)propyl)propane-1,3-diamine (bmdpt)

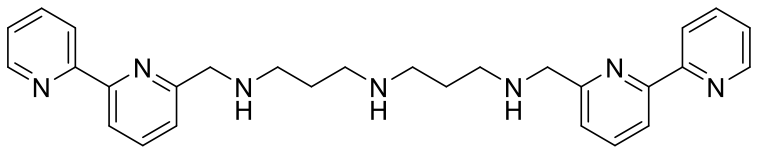

figure 22: The chemical structure of bmdpt.

A solution of 2,2'-bipyridine-6-carbaldehyde (1.10 g, 5.97 × 10^{-3} mol) and bis(3-aminopropyl)amine (0.40 mL, 2.9 × 10^{-3} mol) in methanol (78 mL) was refluxed for two hours with constant stirring. The reaction mixture was cooled to room temperature, and $NaBH_4$ (0.32 g, 8.5 × 10^{-3} mol) was added slowly to the reaction mixture, which caused effervescence. After stirring for a further 2 h the mixture was filtered through celite, the filter pad was washed with methanol (30 mL), and the combined filtrates were reduced to dryness (rotavap), yielding a yellow residue. Deionised water (20 mL) was added, and the mixture was extracted with chloroform (3 × 20 mL). The combined organic layers were dried over anhydrous Na_2SO_4, the mixture was filtered, and the filtrate was reduced to dryness (rotavap). The product was obtained as dark yellow oil (2.28 g, 81.72% based on 2,2'-bipyridine-6-carbaldehyde). ^{1}H NMR (400 MHz, $CDCl_3$): δ 8.64 (dq, 2H, H14), 8.40 (dt, 2H, H11), 8.23 (dd, 2H, H8), 7.77 (m, 4H, H13/H7), 7.26 (t, 6H, H6/H12),

3.95 (s, 4H, H4), 2.69 (tt, 8H, H1/H3), 1.73 (m, 4H, H2); ^{13}C NMR (101 MHz, $CDCl_3$): δ 159.4 (C9), 156.4 (C10), 155.6 (C5), 149.2 (C14), 137.3 (C7), 136.9 (C13), 123.7 (C12), 122.3 (C6), 121.2 (C11), 119.3 (C8), 55.3 (C4), 48.6 and 48.1(C1/3), 30.6 (C2). HRESI-MS: Calculated (*m/z*) for $C_{28}H_{34}N_7^+$ $[M+H]^+$ (*m/z*) = 468.2870, found (*m/z*) for 468.2871; calculated (*m/z*) for $C_{28}H_{35}N_7^{2+}$ $[M+2H]^{2+}$ (*m/z*) =234.6470; found (*m/z*) for 234.6472.

2.2.7 Preparation of bmdpt.3HCl

0.500 g of bmdet was dissolved in 1 M HCl (50 mL) and reduced to dryness (rotavap) to give a pale-yellow solid. To this was dissolved in 20 mL of ethanol and reduced to dryness (rotavap). This was repeated three times, yielding bmdet.3HCl as a pale-pink solid (0.506 g).

2.3 Complex precursor synthesis

2.3.1 Sodium tris-carbonatocobaltate(III) trihydrate, ($Na_3[Co(CO_3)_3].3H_2O$)

This was synthesized using a modified method of *Bauer and Drinkard*.[39]

To a solution of cobalt nitrate hexahydrate ($Co(NO_3)_2.6H_2O$, 29.1 g, 0.10 mol) in deionised water (50 mL) was added 30% H_2O_2 (10 ml, excess). The resulting solution was then added to an ice-cold slurry of sodium bicarbonate (42.0 g, 0.50 mol) in deionised water (50 mL) with constant stirring, resulting in a deep green solution. After addition was complete, the reaction mixture was stirred at 0°C for 1 h. The olive-green solution was filtered and washed with cold deionised water (3 × 10 mL), then washed with absolute alcohol. The product was obtained as a fine olive-green powder (34.56 g, 95.48% based on $Co(NO_3)_2.6H_2O$).

2.4 Preparation of bmdet complexes

Caution: Perchlorate salts are potentially explosive. Care was taken to use a low temperature while reducing volumes by rotary evaporator, and solutions were never taken to absolute dryness in this case.

2.4.1 $[Co_2(bmdet)_2Cl](ClO_4)_5$

To a solution of bmdet.3HCl (1.42 g, 2.59×10^{-3} mol) in deionised water (10 mL) was added $Na_3[Co(CO_3)_3].3H_2O$ (0.92 g, 2.5×10^{-3} mol), resulting in a green solution. The reaction mixture was heated at 65°C for 5 min, during which CO_2 evolved, and the solution turned dark red. The reaction mixture was filtered through celite, and the filter pad was washed with deionised water (3 × 10 mL). The combined filtrates were diluted to 400 mL with deionised water and loaded onto a

Dowex 50W-X2 cation exchange column. A minor light pink band eluted with 3 M HCl and was discarded, while a dark orange band was obtained on elution with 5 M HCl. This was reduced to dryness (rotavap), yielding an orange, sticky solid.

The dried complex was dissolved in the minimum volume (3-4 mL) of deionised water and addition of a small amount of solid sodium perchlorate gave an orange precipitate. The mixture was cooled in an ice bath, the orange solid was removed by filtration and washed with iso-propanol. Attempts to obtain X-ray quality crystals from slow cooling of a hot, concentrated aqueous solution of the product were unsuccessful. HRESI-MS: Calculated (*m/z*) for $CoC_{26}H_{29}N_7^{2+}$ $[M]^{2+}$ (*m/z*) =249.0900; found (*m/z*) = 249.0903

2.4.2 [Cu(bmdet)](ClO$_4$)$_2$

Copper(II) perchlorate hexahydrate (0.17 g, 4.5×10^{-4} mol) was added to a solution of bmdet (0.20 g, 4.5×10^{-4} mol) in deionised water (2 mL), resulting in a blue solution that gave a green, sticky solid on standing. The reaction mixture was warmed to dissolve the solid, and the mixture was then filtered through cotton wool. On standing of the filtrate overnight, polycrystalline material was obtained that was unsuitable for X-ray structural characterisation. HRESI-MS: Calculated (*m/z*) for $CuC_{26}H_{29}N_7^{2+}$ $[M]^{2+}$ (*m/z*) =251.0880; found (*m/z*) = 251.0885.

2.4.3 [Mn(bmdet)](ClO$_4$)$_2$

Manganese(II) perchlorate hexahydrate (0.16 g, 4.5×10^{-4} mol) was added to a solution of bmdet (0.20 g, 4.5×10^{-4} mol) in deionised water (2 mL), which instantly turned into yellow precipitates. Attempts to obtain X-ray quality crystals from slow cooling of a hot, concentrated aqueous solution of the product were unsuccessful. HRESI-MS: Calculated (*m/z*) for $MnC_{26}H_{29}N_7ClO_4^+$ $[M]^+$ (*m/z*) = 593.1340, found (*m/z*) = 593.1343; Calculated (*m/z*) for $MnC_{26}H_{29}N_7^{2+}$ $[M]^{2+}$ (*m/z*) =247.0930, found (*m/z*) = 247.0927.

2.4.4 [Fe(bmdet)](ClO$_4$)$_2$

Iron (II) perchlorate hydrate (0.16 g, 4.5×10^{-4} mol) was added to a solution of bmdet (0.20 g, 4.5×10^{-4} mol) in methanol. The mixture turned deep purple and a sticky solid was formed. The reaction mixture was warmed to dissolve the solid, and the mixture was then filtered through cotton wool. Slow cooling of the warm filtrate overnight failed to give X-ray quality crystals. HRESI-MS: Calculated (*m/z*) for $FeC_{26}H_{29}N_7^{2+}$ $[M]^{2+}$ (*m/z*) =246.5830; found (*m/z*) = 246.5833.

2.4.5 [Cu(bmdet)](CH$_3$COO)$_2$

Copper (II) acetate monohydrate (0.090 g, 4.5×10^{-4} mol) was added to a solution of bmdet (0.20 g, 4.5×10^{-4} mol) in methanol (5 mL). The reaction mixture was heated for 10 min. and turned dark green. Slow cooling of the reaction mixture failed to give X-ray quality crystals. Calculated (*m/z*) for $CuC_{26}H_{28}N_7^+$ $[M]^+$ (*m/z*) = 501.1700, found (*m/z*) = 501.1695; Calculated (*m/z*) for $CuC_{26}H_{29}N_7^{2+}$ $[M]^{2+}$ (*m/z*) =251.0880, found (*m/z*) = 251.0884.

2.4.6 [Zn(bmdet)](ClO$_4$)$_2$

Zinc (II) perchlorate hexahydrate (0.088 g, 4.5×10^{-4} mol) was added to a solution of bmdet (0.20 g, 4.5×10^{-4} mol) in deionised water (2 mL). A white precipitate was formed, which was filtered and washed with ice-cold deionised water. The obtained precipitate was dissolved in the minimum volume of deionised water, heated, and then slowly cooled to attempt crystallisation, which was unsuccessful. HRESI-MS: Calculated (*m/z*) for $ZnC_{26}H_{29}N_7^{2+}$ $[M]^{2+}$ (*m/z*) =251.5880; found (*m/z*) = 251.5882.

2.4.6 [Rh(bmdet)](Cl)$_3$

Rhodium(III) chloride hydrate (0.050 g, 1.6×10^{-4} mol) was added to a solution of bmdet (0.070 g, 1.6×10^{-4} mol) in hot deionised water (5 mL) and the solution was stirred for 1 h. The resulting light brown solution was reduced to low volume (rotavap) and a small amount of sodium perchlorate was added, which gave a beige-coloured precipitate.

2.4.7 [Ru(bmdet)]Cl$_2$

[Ru(DMSO)$_4$Cl$_2$] (0.050 g, 1.0×10^{-4} mol) was added to a solution of bmdet (0.045 g, 1.0×10^{-4} mol) in deionised water (5 mL) the dark red solution was stirred for 1 h. The solution was reduced to dryness (rotavap). Dissolved the complex in a minimum volume of deionised water (2 mL) and added sodium hexafluorophosphate. Light red colour precipitates are obtained, filtered and washed with ice cold water. HRESI-MS: Calculated (*m/z*) for $RuC_{26}H_{29}N_7^{2+}$ $[M]^{2+}$ (*m/z*) =270.5763; found (*m/z*) = 270.5759.

2.5 Preparation of bmdpt complexes

2.5.1 [Co$_2$(bmdpt)$_2$Cl](ClO$_4$)$_5$

To a solution of bmdpt.3HCl (0.506 g, 2.59×10^{-3} mol) in deionised water (10 mL) was added $Na_3[Co(CO_3)_3].3H_2O$ (0.330 g, 2.5×10^{-3} mol), resulting in a green solution. The reaction mixture

was heated at 65°C for 5 min, during which CO_2 evolved, and the solution turned dark red. The reaction mixture was filtered through celite, and the filter pad was washed with deionised water (3 × 10 mL). The combined filtrates were diluted to 200 mL with deionised water and loaded onto a Dowex 50W-X2 cation exchange column. A minor light pink band eluted with 3 M HCl and was discarded, while a dark orange band was obtained on elution with 5 M HCl. This was reduced to dryness (rotavap), yielding an orange, sticky solid.

The dried complex was dissolved in the minimum volume (3-4 mL) of deionised water and addition of a small amount of solid sodium perchlorate gave a pale orange precipitate. Heated the precipitates to dissolve. Attempts to obtain X-ray quality crystals from slow cooling of a hot, concentrated aqueous solution of the product were unsuccessful.

2.6 Solution Studies

2.6.1 Job's plots

Reaction of bmdet and bmdpt with $[Cu(OH_2)_6](ClO_4)_2$

Stock solutions were prepared as follows

Solution A - 0.012 M $[Cu(OH_2)_6](ClO_4)_2$ in CH_3CN

Solution B - 0.012 M bmdet in CH_3CN

Solution C – 0.012 M bmdpt in CH_3CN

All solutions were freshly prepared.

Using an automatic pipette, 0, 0.50, 1.00, 1.50, 2.00, 2.50, 3.00, 3.50, 4.00, 4.50, and 5.00 mL of the ligand solution was added to separate 5 mL volumetric flasks. Then, 5.00, 4.50, 4.00, 3.50, 3.00, 2.50, 2.00, 1.50, 1.00, 0.50, and 0 mL of the metal solution was added to each flask, to give 11 solutions having varying concentrations of both metal ion and ligand. Each flask was mixed well, and the UV/vis spectrum of each solution was then recorded (800nm to 600nm) after a few minutes, using CH_3CN as the baseline.

A graph of specific absorbance versus mole fraction of the metal was plotted using the collected data.

Reaction of bmdet and bmdpt with $[Co(OH_2)_6](ClO_4)_2$

Stock solutions were prepared as follows.

Solution A - 0.0030 M $[Co(OH_2)_6](ClO_4)_2$ in CH_3CN

Solution B - 0.0030 M bmdet in CH_3CN

Solution C - 0.0030 M bmdpt in CH_3CN

All solutions were freshly prepared.

Solutions were prepared and UV/Vis spectra obtained as described in Section 1.6.1 above.

A graph of specific absorbance versus mole fraction of the metal was plotted from the collected data.

2.6.2 Mass spectroscopy

Solution A - 0.0114M $[M(OH_2)_6](ClO_4)_2$ in CH_3CN and MeOH; M = Co, Cu, Ni, Zn, Mn, and Fe].

Solution B - 0.0114M bmdet in CH_3CN and MeOH.

Solution C - 0.0114M bmdpt in CH_3CN and MeOH.

The mass spectrometry samples were prepared by mixing the ligand solution with 1, 2, or 3 equivalents of the metal ion solutions. Specifically, 1, 2, and 3 equivalents of solution A were added to 50 μL of solutions B and C, respectively. The resulting metal–ligand mixtures were thoroughly mixed and allowed to stand at room temperature. For mass spectrometric analysis, 2 μL of each equilibrated solution was diluted with 1.0 mL of a CH_3CN or MeOH, and each sample was then directly injected into the mass spectrometer.

The observed spectrum was compared with the calculated spectrum which was obtained from Molecular Mass Calculator.[40]

3. Results and discussion

3.1 Ligand synthesis

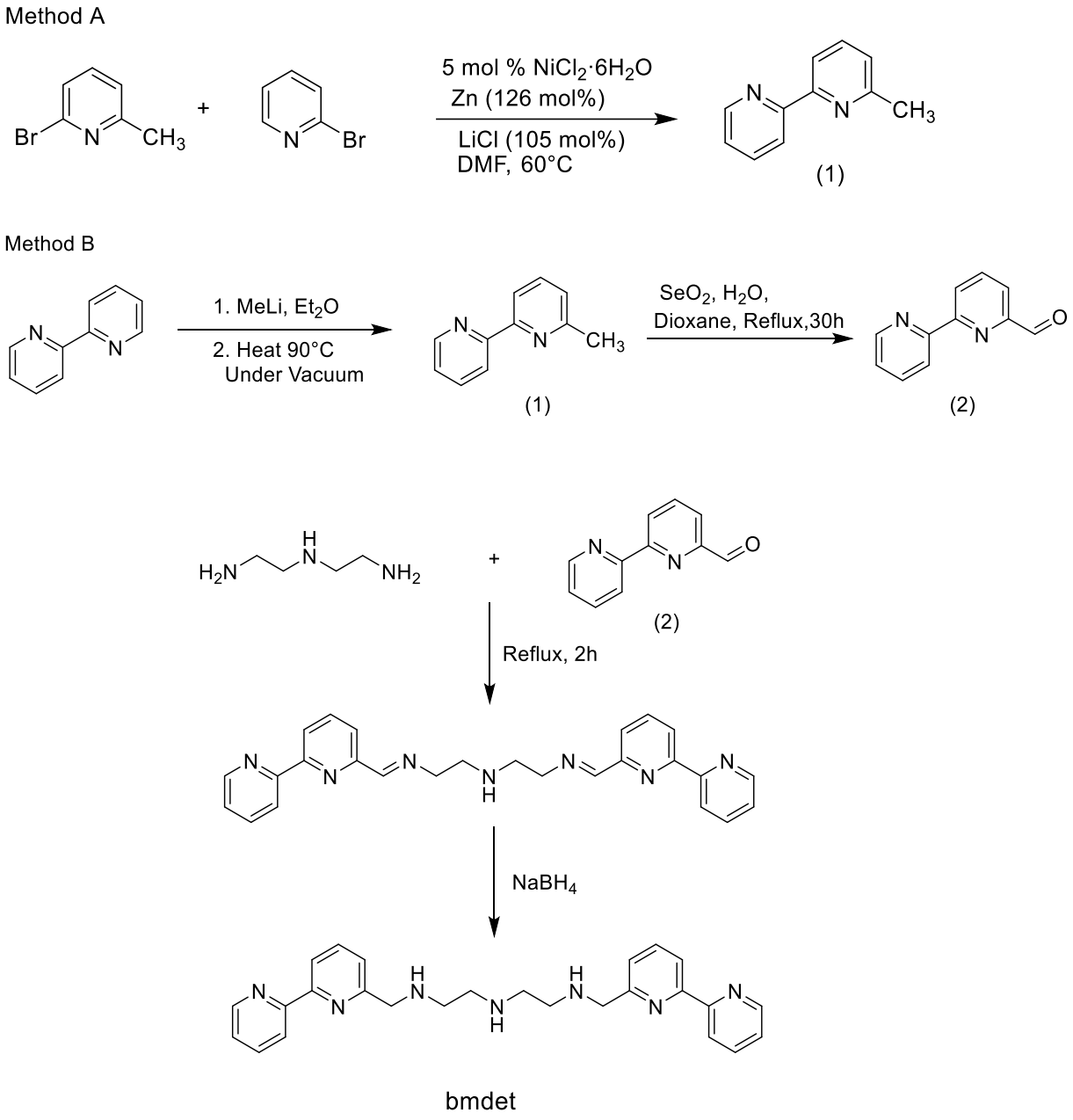

Scheme 1: The synthetic route for the preparation of bmdet.

Scheme 1 shows the synthetic route followed for the synthesis of the new ligand, bmdet. This involves reaction of 2,2'-bipyridine-6-carbaldehyde with diethylenetriamine and reduction of the

resulting diimine with $NaBH_4$. 2,2'-bipyridine-6-carbaldehyde was prepared by SeO_2 oxidation of 6-methyl-2,2'-bipyridine, which was itself prepared from 2,2'-bipyridine by reaction with MeLi.

Synthesis of the ligand precursor, 6-methyl-2,2'-bipyridine (1), was first attempted using method A, a modified version of the method reported by Liao *et al*.[36] This involves Ni-catalysed reductive coupling of heteroaryl bromides, in which Zn-LiCl acts as a reducing agent. 2-bromo-6-methylbipyridine and 2-bromopyridine were reacted in the presence of $NiCl_2.6H_2O$, excess lithium chloride and zinc dust in hot dimethylformamide, as described in Chapter 2. This method of synthesis of 6-methyl-2,2'-bipyridine was attempted at least 4 times. Purification of the crude product via column chromatography on both silica gel and alumina, with different solvent combinations as mobile phases, was attempted, but the pure product could not be obtained. Analysis by mass spectrometry gave a product ion peak at *m/z* = 171.0916, consistent with the calculated value for 6-methyl-2,2'-bipyridine (calculated for $C_{11}H_{11}N_2^+$ $[M+H]^+$ (*m/z*) = 171.0920; found m/z = 171.0916). However, the presence of several other peaks suggested the presence of additional compounds. Further analysis of the compound by ^1H NMR spectroscopy revealed a noisy spectrum, consistent with the presence of multiple compounds. At this point, it was decided not to continue with the reported procedure. Thus, Method B was utlised to synthesise 6-methyl-2,2'-bipyridine.

Method B for the synthesis of 6-methyl-2,2'-bipyridine uses a modified method of Schmalzl and Summers[37] which involves a nucleophilic addition-aromatisation sequence. This method contrasts with the previously attempted reductive dimerization by utilizing the pre-formed bipyridine backbone for functionalization. The route starts from the commercially available 2,2'-bipyridine, which was C-methylated by MeLi. In this reaction, methyl lithium acts as a strong nucleophile and base. When added to the solution of 2,2'-bipyridine, it attacks the electron-deficient pyridine ring, specifically at the position ortho to the nitrogen (the 6-position). This results in the formation of a dihydropyridine intermediate, indicated by the deep red coloration of the reaction mixture. Quenching the reaction mixture with crushed ice protonates this intermediate, yielding a reduced, non-aromatic species, as indicated by the observed yellow colour. Subsequent heating at 90 °C under reduced pressure restores aromaticity through dehydrogenation, yielding the desired 6-methyl-2,2′-bipyridine. Purification by column chromatography on alumina (initial elution with dichloromethane/toluene (50:50), then with dichloromethane (100%)), afforded the product as a

light-yellow oil. The product was characterised by High-Resolution Electrospray Ionization Mass Spectrometry and Nuclear Magnetic Resonance spectroscopy. The observed molecular ion peak at *m/z* = 171.0916 ($[M+H]^+$) (figure 26) closely matches the calculated value for $C_{11}H_{11}N_2^+$ (*m/z* = 171.0920), confirming the expected molecular formula. Further structural confirmation was obtained from NMR spectroscopy. The ^1H (figure 24) and ^{13}C (figure 25) spectra of the product are consistent with its formulation. The molecule lacks symmetry owing to the methyl functional group, and therefore, all protons and carbon atoms have different chemical environments. The ^1H NMR spectrum shows a singlet at δ 2.53 ppm integrating for three protons, which is assigned to a methyl group attached to an aromatic carbon. This chemical shift is consistent with a methyl group deshielded by the adjacent aromatic system. The remaining one proton signals between δ 7.05 and 8.57 ppm correspond to seven aromatic protons of the bipyridine framework. The most downfield resonance (δ 8.57 ppm) arises from the proton (H-6') adjacent to a nitrogen atom, reflecting its deshielded environment. The multiplets in the regions δ 7.79 – 7.62 ppm, δ 7.62 – 7.51 ppm, and δ 7.20 – 7.10 ppm correspond to the remaining aromatic protons on both rings, showing complex coupling patterns typical of a bipyridine system. The doublet at δ 7.05 ppm can be assigned to the proton at the 5-position. The ^{13}C NMR spectrum displays eleven carbon signals, ten in the aromatic region and one in the aliphatic region), consistent with the proposed structure. The low intensity signals in the range δ 155.6 – 157.9 ppm are assigned to the three quaternary carbons adjacent to nitrogen atoms present in the molecule, while resonances between δ 118.1 and 149.1 ppm correspond to the remaining aromatic carbons. A single aliphatic carbon signal at δ 24.66 ppm confirms the presence of the methyl substituent.

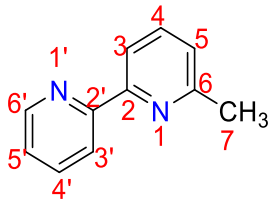

figure 23: The chemical structure and atom numbering scheme of 6-methyl-2,2'-bipyridine.

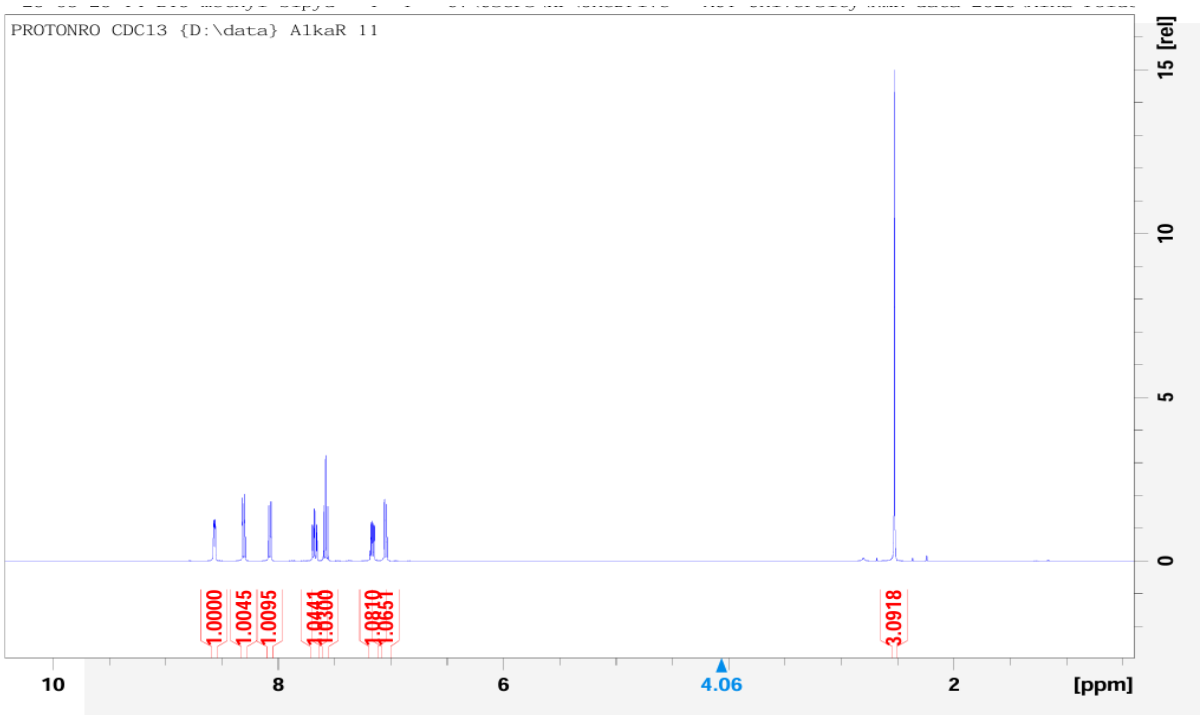

figure24: The ^{1}H NMR spectrum of 6-methyl-2,2′-bipyridine in $CDCl_3$

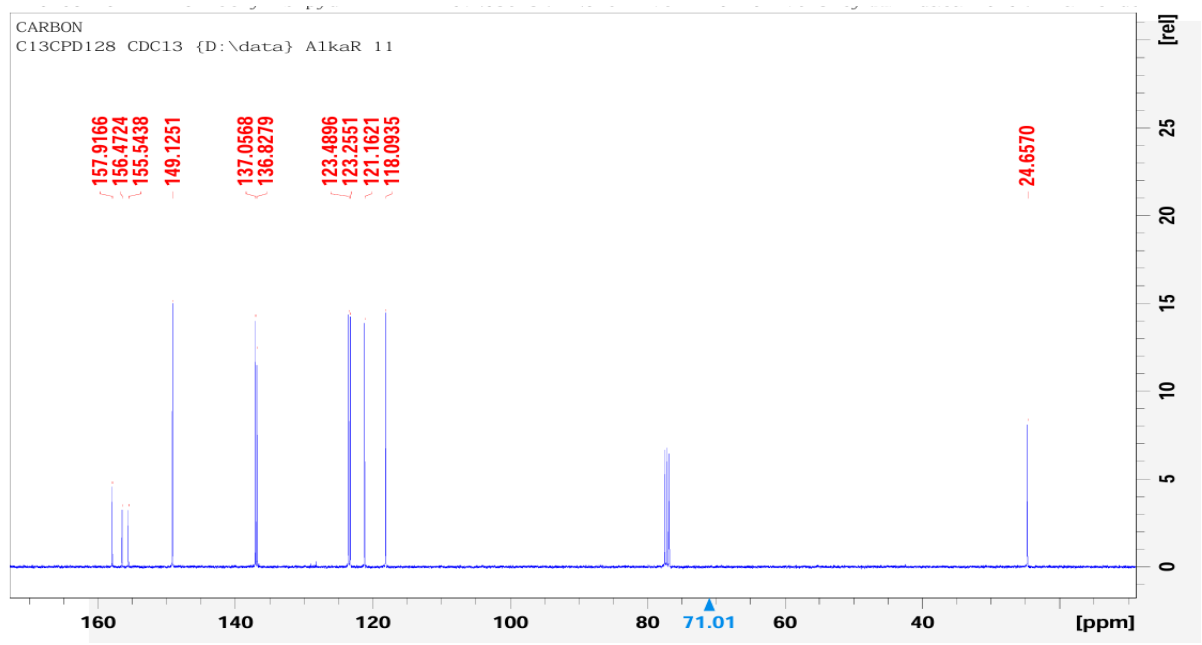

figure 25: The ^{13}C NMR spectrum of 6-methyl-2,2′-bipyridine in $CDCl_3$

figure 26: The Mass Spectrum of 6-methyl-2,2'-bipyridine in $CDCl_3$.

2,2'-bipyridine-6-carbaldehyde was synthesized using a modified method of Heirtzler *et al*. by the oxidation of 6-methyl-2,2'-bipyridine. This is a modified Riley oxidation, a method for oxidizing methyl groups adjacent to aromatic systems to aldehydes or carboxylic acids, which typically employs selenium dioxide as the oxidizing agent. The initial step involves refluxing 6-methyl-2,2'-bipyridine with selenium dioxide in a dioxane/water mixture under an N_2 atmosphere. Selenium dioxide is known to selectively oxidize allylic and benzylic positions. In this case, the methyl group is benzylic to the pyridine ring, forming an aldehyde while selenium dioxide is reduced to elemental selenium, which was observed experimentally which was removed by filtration through celite. The long reflux time (26 h) and staged addition of selenium dioxide and water were employed to ensure complete oxidation while limiting over-oxidation to the corresponding carboxylic acid. The product was obtained as a dark yellow oil that solidified to give a pale orange solid on standing overnight. The formed product was identified by High-Resolution Electrospray Ionization Mass Spectrometry and Nuclear Magnetic Resonance spectroscopy. The observed molecular ion peak at *m/z* 185.0709 ($[M+H]^+$) matches very closely with the calculated value of *m/z* 185.0710 for $C_{11}H_9N_2O^+$. This excellent agreement confirms the molecular formula of the aldehyde and supports successful oxidation of the methyl group to a formyl group without further oxidation. The ^1H NMR spectrum further supports the formation of the aldehyde. The molecule lacks symmetry owing to the aldehyde functional group, and therefore,

all protons and carbon atoms have different chemical environments. The signal at δ 10.18 ppm (1H, H-7) is characteristic of an aldehydic proton; it is strongly deshielded due to the adjacent carbonyl group. The remaining signals between δ 8.7 and 7.3 ppm correspond to the aromatic protons of the 2,2′-bipyridine framework. Protons located close to the nitrogen atoms appear at higher chemical shifts (δ 8.6–8.7 ppm) due to the electron-withdrawing effect of the pyridine nitrogen atoms, while protons further away resonate at slightly lower chemical shifts (from δ 8.56 to 7.33 ppm). The ^{13}C NMR spectrum was consistent with the proposed structure. The total number and chemical shift distribution of carbon signals are fully consistent with a mono-aldehyde-substituted 2,2′-bipyridine system. The resonance at δ 194.1 ppm is assigned to the aldehyde carbonyl carbon. The three low intensity signals between δ 157.0 and 152.7 ppm correspond to quaternary carbons directly bonded to nitrogen in the pyridine rings, which are deshielded by the electronegative nitrogen atoms. The remaining aromatic carbon signals observed between δ 149.7 and 121.6 ppm are assigned to the substituted and unsubstituted carbons of the bipyridine rings.

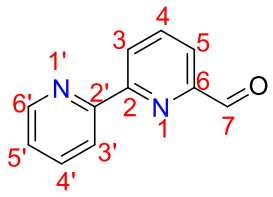

figure 27: The chemical structure and atom numbering scheme of 2,2′-bipyridine-6-carbaldehyde.

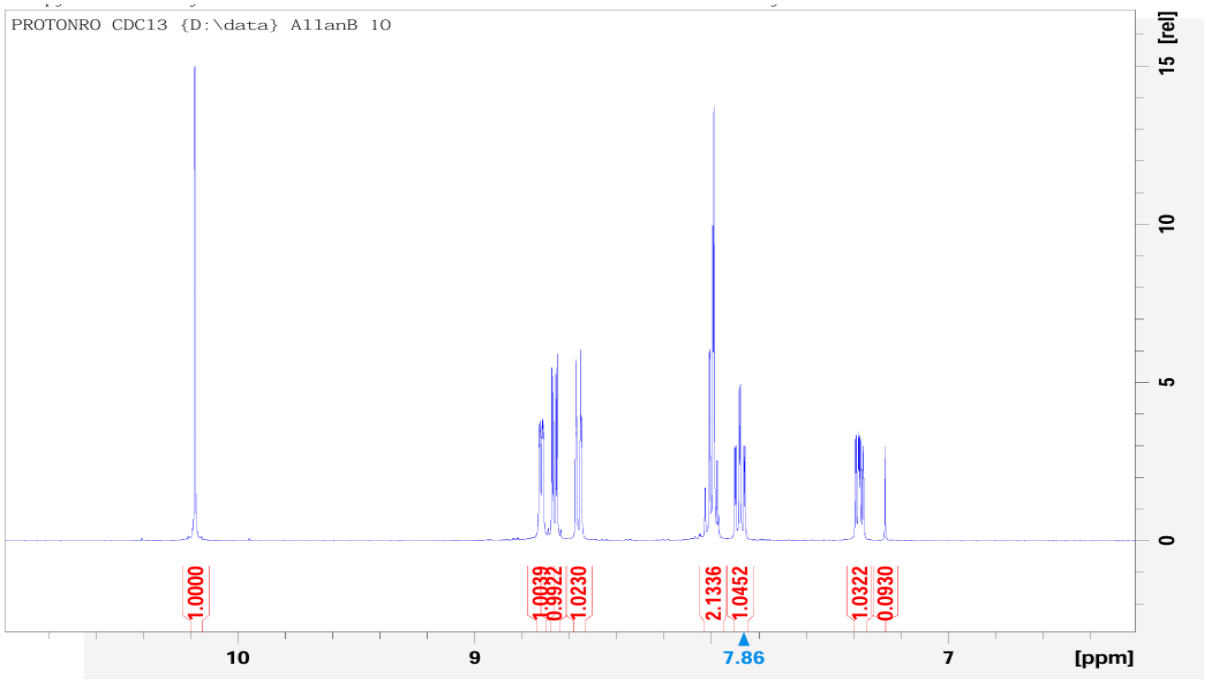

figure 28: The ^{1}H NMR spectrum of 2,2′-bipyridine-6-carbaldehyde in $CDCl_3$

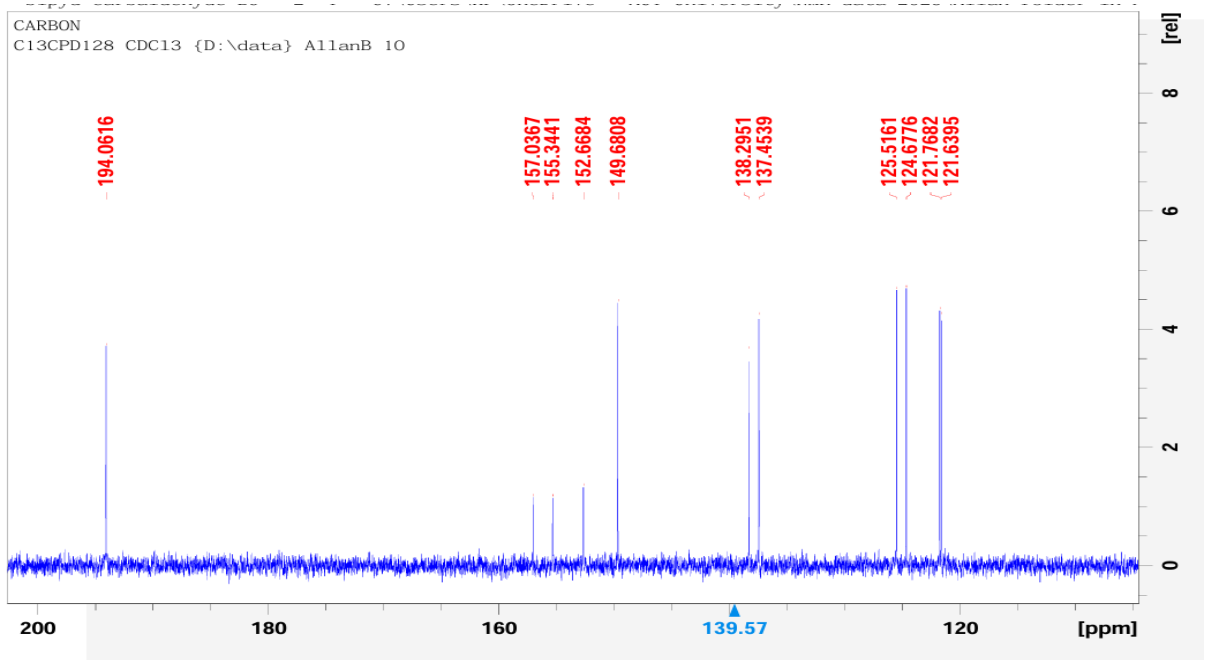

figure 29: The ^{13}C NMR spectrum of 2,2′-bipyridine-6-carbaldehyde in $CDCl_3$

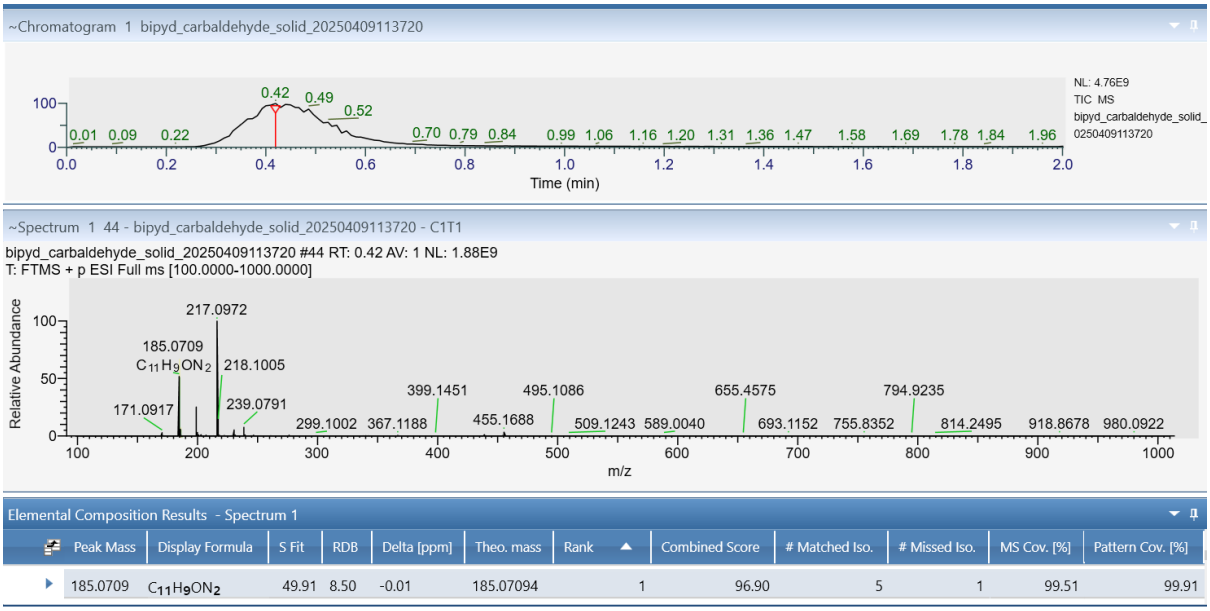

figure 30: The Mass Spectrum of 2,2′-bipyridine-6-carbaldehyde.

The bmdet (the abbreviation comes from **b**ipyridyl**me**thyl**die**thylene**t**riamine) ligand was prepared from the reductive amination of 2,2′-bipyridine-6-carbaldehyde with diethylenetriamine in methanol. In the first step, 2,2'-bipyridine-6-carbaldehyde was reacted with diethylenetriamine in refluxing methanol for two hours. This involves a condensation reaction between the aldehyde functional group of the bipyridine derivative and the primary amine groups of diethylenetriamine, resulting in the formation of a diimine intermediate containing two C=N double bonds and elimination of water. After cooling the reaction mixture to room temperature, sodium borohydride ($NaBH_4$) was added gradually to reduce the imines to secondary amines (C–NH) via hydride transfer. After an aqueous workup to remove inorganic impurities, and extraction into chloroform, the bmdet ligand was isolated as a dark yellow oil in moderate yield.

The new ligand was characterised by High-Resolution Electrospray Ionization Mass Spectrometry and Nuclear Magnetic Resonance spectroscopy. HRESI-MS confirms the molecular composition of the bmdet ligand. The observed molecular ion peak at m/z = 440.2556 corresponds to the calculated value for $[C_{26}H_{30}N_7]^+$ (m/z = 440.2560), the singly protonated ligand, confirming the expected molecular weight. In addition, a peak corresponding to the doubly charged ion at m/z = 220.6215 is also observed (calculated $[C_{26}H_{31}N_7]^{2+}$ (m/z = 220.6310)) (figure 34). The presence of both singly and doubly protonated species is typical for polyamine ligands and further supports the successful formation of the desired ligand.

The bmdet molecule is symmetrical about the central N atom, and as a result exhibits relatively simple NMR spectra. The ^{1}H NMR spectrum of bmdet (figure 32) exhibits signals in both the aromatic and aliphatic regions, the former corresponding to the pyridine protons, and the latter the methylene protons in the molecule. The peak at δ 8.67 (dq, 2H) is assigned to H13, while that at δ 8.43 (dt, 2H) corresponds to H10. The doublet at δ 8.26 (2H) is attributed to H7, while the peaks at δ 7.78 (2H, td) and δ 7.75 (2H, t) overlap somewhat; the former is due to H12 and the latter to H6. The multiplet centred at δ 7.27 (nominally 6H, but effectively 4H due to chloroform solvent overlap) is assigned to H5 and H11. In the aliphatic region, the singlet at δ 3.99 (4H) corresponds to the isolated H3 methylene protons that are directly adjacent to nitrogen atoms in the diethylenetriamine backbone, with the chemical shift reflecting their deshielded environment due to the electronegativity of nitrogen. The broad multiplet at δ 2.83 (8H) is assigned to the H1 and H2 methylene protons.

The bmdet molecule exhibits thirteen peaks in the ^{13}C NMR (figure 33), ten of which lie in the aromatic region (δ 159.3 - 119.2) and three in the aliphatic (δ 55.1 - 49.2). The three aromatic peaks at lowest field are of significantly lower intensity than the others, suggesting that these signals are due to carbon atoms C4, C8 and C9 of the bipyridine moieties that do not bear a hydrogen atom. The peak at δ = 55.1 corresponds to C3, while the remaining aliphatic peaks at δ = 49.6 and δ = 49.2 arise from C1 and C2. Thus the full assignments are δ = 159.3, C8; δ = 156.3, C9; δ = 155.5, C4; δ = 149.3, C13; δ = 137.3, C6; δ = 136.8, C12; δ =123.6, C11; δ = 122.2, C5; δ =121.1, C10; δ = 119.2, C7; δ = 55.1, C3; δ = 49.6, 49.2; C1/2.

The above assignments are made on the basis of analysis of the 2D NMR spectra (COSY, HSQC, and HMBC). The COSY spectrum reveals coupling patterns that distinguish overlapping aromatic protons. The HSQC spectrum correlates proton signals to their directly attached carbons, confirming assignments of all the protonated carbon atoms. HMBC correlations help assign the three quaternary carbons by their long-range couplings to protons in the aromatic rings. For example, the ^{13}C peaks at δ = 156.3 and 155.5 must be due to carbons C4 and C9 as no correlation to the H3 protons is observed for these signals. This means the ^{13}C peak at δ = 159.3 can be assigned to C8. Similar reasoning requires the peak at δ = 122.2 to be due to C5. The HSQC spectrum is then used to assign H5, and the COSY spectrum then shows H5 coupling to H6, thus assigning both H6 and C6. H7 and C7 are assigned similarly. H13 is always at lowest field in 2-

substituted pyridines, and knowing this allows assignment of all the protons and carbons in this ring. Hence, the ^{1}H and ^{13}C NMR peaks for the bmdet molecule can be assigned, with the exception of C/H1 and C/H2, which cannot be uniquely determined.

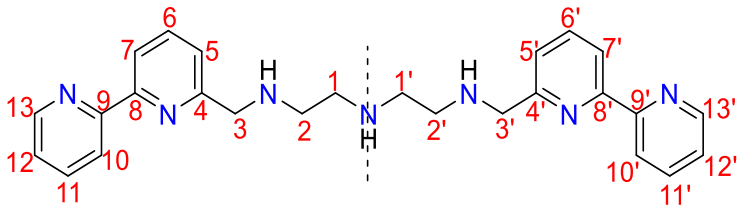

figure 31: The chemical structure and atom numbering scheme of bmdet

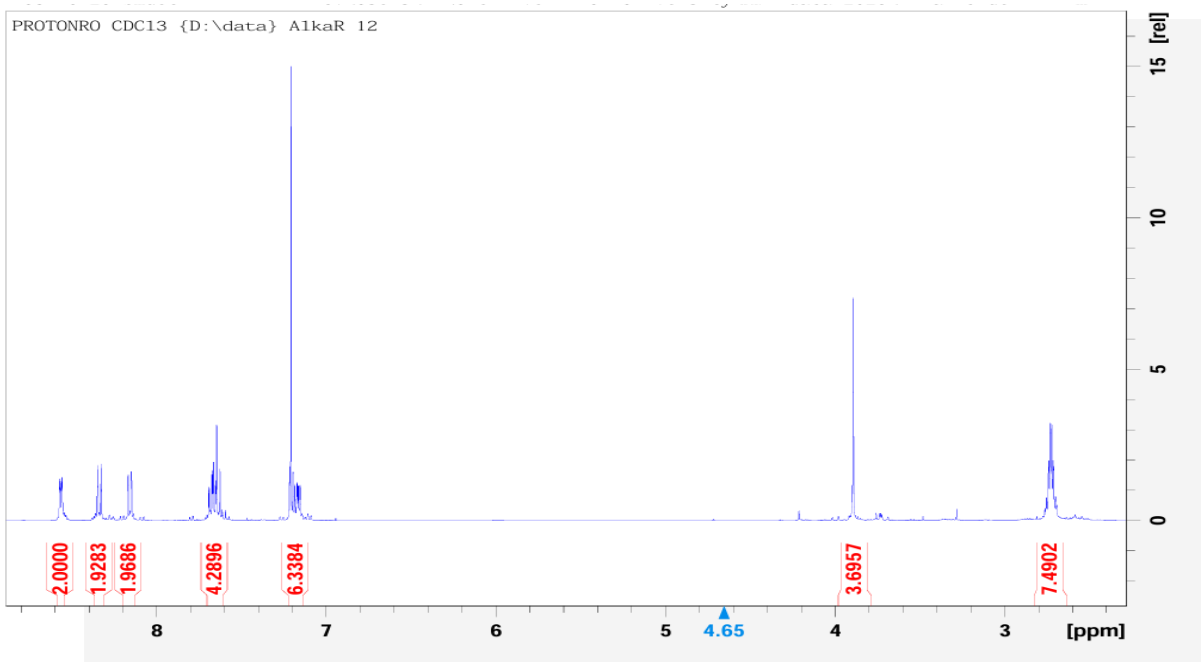

figure 32: The ^{1}H NMR spectrum of bmdet in $CDCl_3$

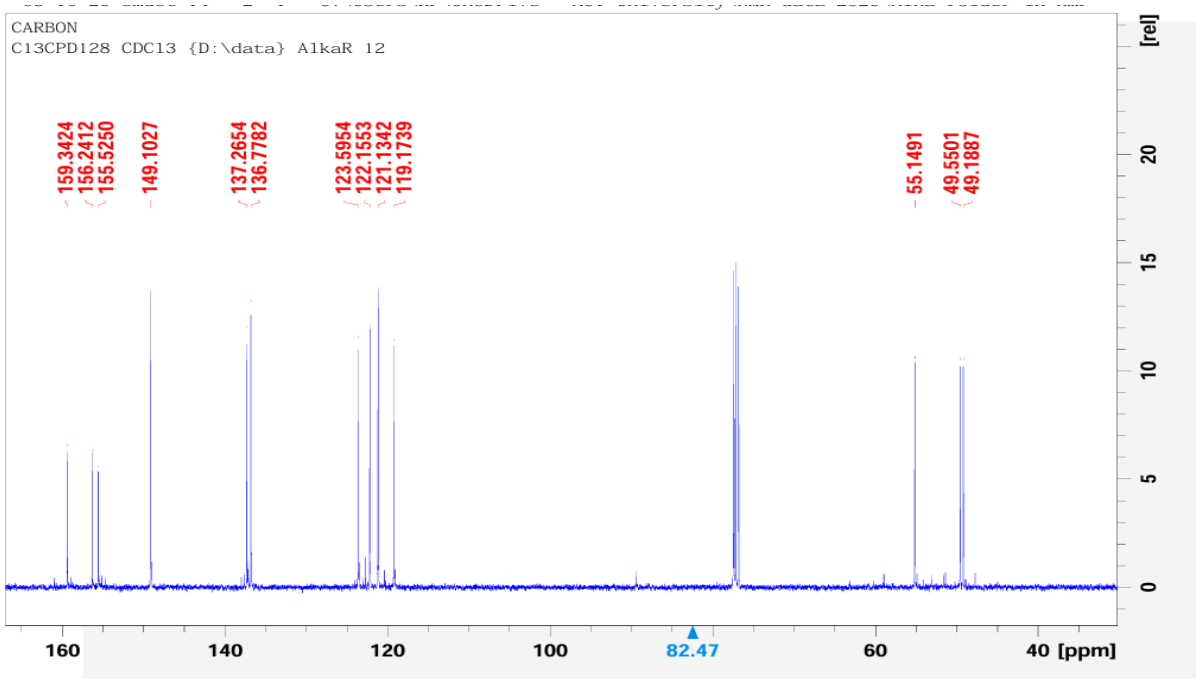

figure 33: The ^{13}C NMR spectrum of bmdet in $CDCl_3$

figure 34: The Mass Spectrum of bmdet.

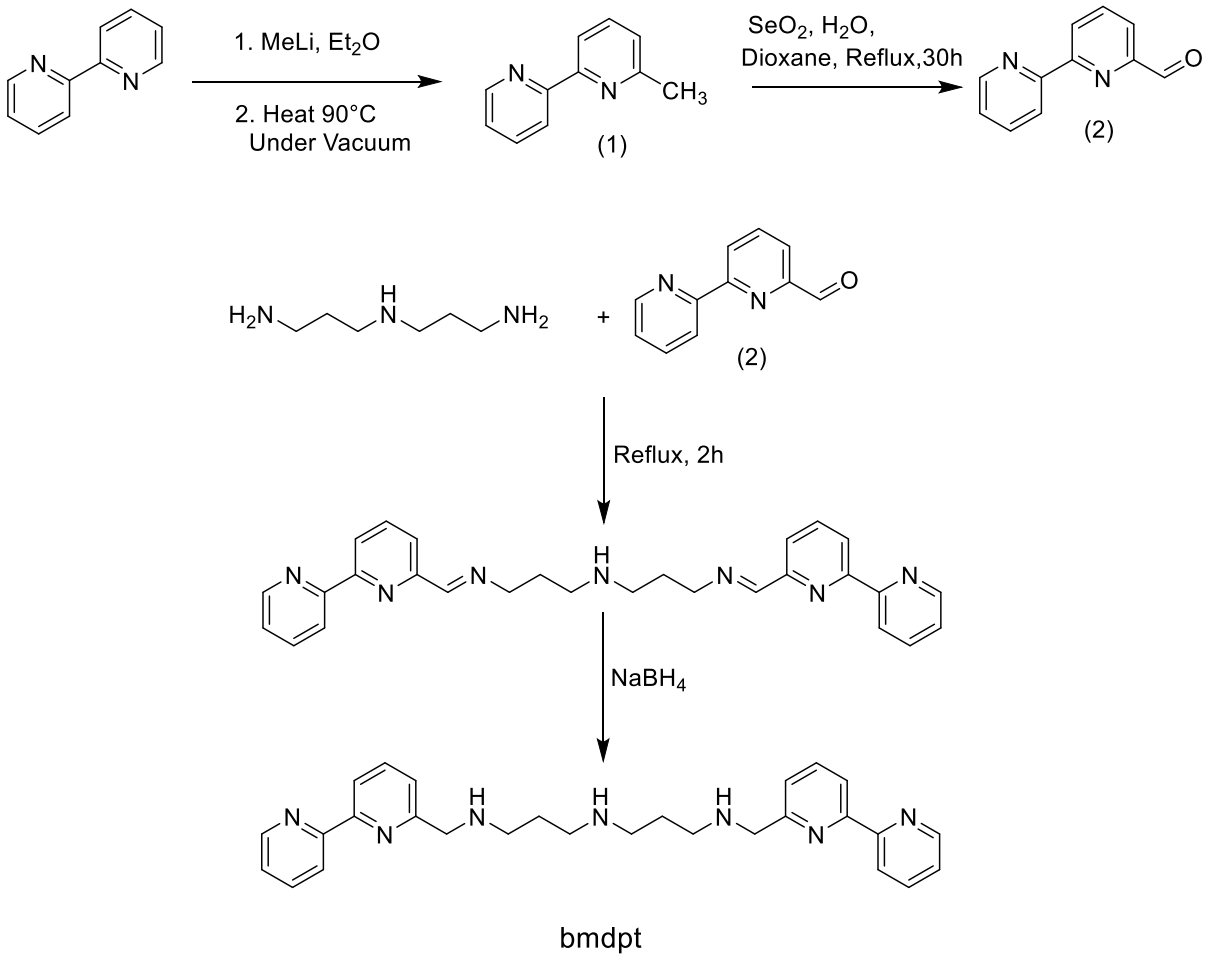

Scheme 2: The synthetic route for the preparation of bmdpt

Scheme 2 shows the synthetic route followed for the synthesis of the new ligand, bmdpt. This ligand is synthesised in the same manner as bmdet. The ligand was prepared from the reductive amination of 2,2'-bipyridine-6-carbaldehyde with bis(3-aminopropyl)amine in methanol as solvent. $NaBH_4$ was used as the reducing agent. The bmdpt ligand was isolated as an oil and was characterised by High-Resolution Electrospray Ionization Mass Spectrometry and Nuclear Magnetic Resonance spectroscopy.

The formed product was identified by High-Resolution Electrospray Ionization Mass Spectrometry and Nuclear Magnetic Resonance spectroscopy. HRESI-MS confirms the molecular composition of the bmdpt ligand. The observed molecular ion peak at *m/z* = 468.2871 corresponds to the calculated value for monoprotonated $[C_{28}H_{34}N_7]^+$ (*m/z* = 468.2870), confirming the expected molecular weight. In addition, the doubly charged ion at *m/z* = 234.6472 matches well with the

calculated $[C_{28}H_{34}N_7]^{2+}$ (*m/z* = 234.6470) (figure 38). The presence of both singly and doubly protonated species is typical for polyamine ligands and further supports the successful formation of the desired ligand.

This ligand contains a mirror plane that makes the bipyridine carbon atoms equivalent to their corresponding counterparts.

The ^{1}H NMR spectrum (figure 36) of the bmdpt ligand appears extremely similar to that of bmdet. This is to be expected, as the two molecules differ only by two -CH_2- groups. Hence, the chemical shifts and coupling of the peaks are essentially identical between the two spectra, except for the appearance of a new four-proton quintet at δ = 1.73 ppm, which is assigned to the H2 protons; the relatively low chemical shift is consistent with the positioning of these protons as far as possible from the electronegative N atoms.

The ^{13}C NMR spectrum (figure 37) is also very similar to that of bmdet, exhibiting fourteen distinct carbon resonances consistent with a symmetrical molecule, with 10 signals in the aromatic region and four in the aliphatic. The peak assignments are the same as for bmdet, with the exception of the new peak at δ = 30.6, which is assigned to C2.

The NMR data are consistent with the proposed structure given in figure 14.

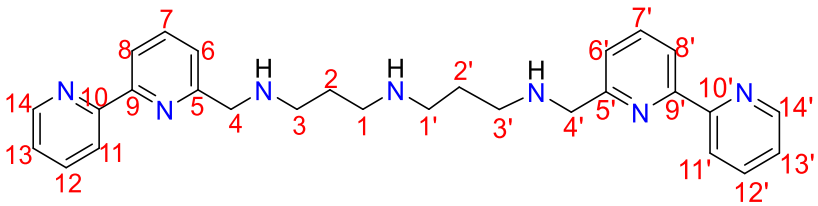

figure 35: The chemical structure and atom numbering scheme of bmdpt.

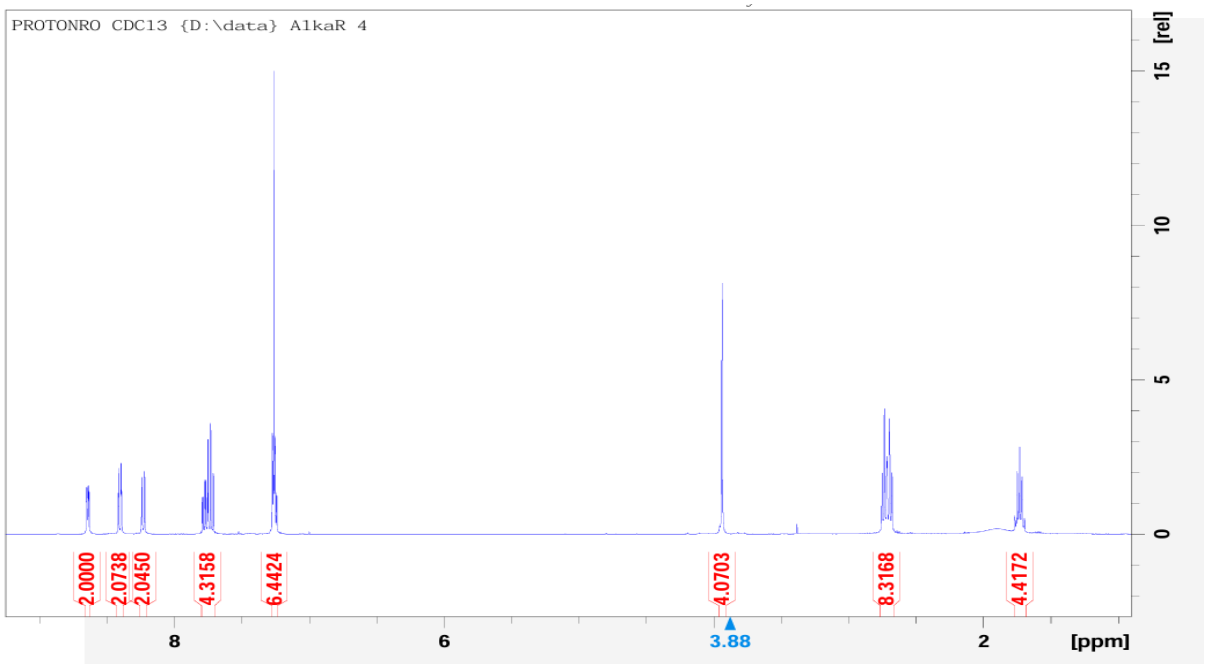

figure 36: The ^{1}H NMR spectrum of bmdpt in $CDCl_3$

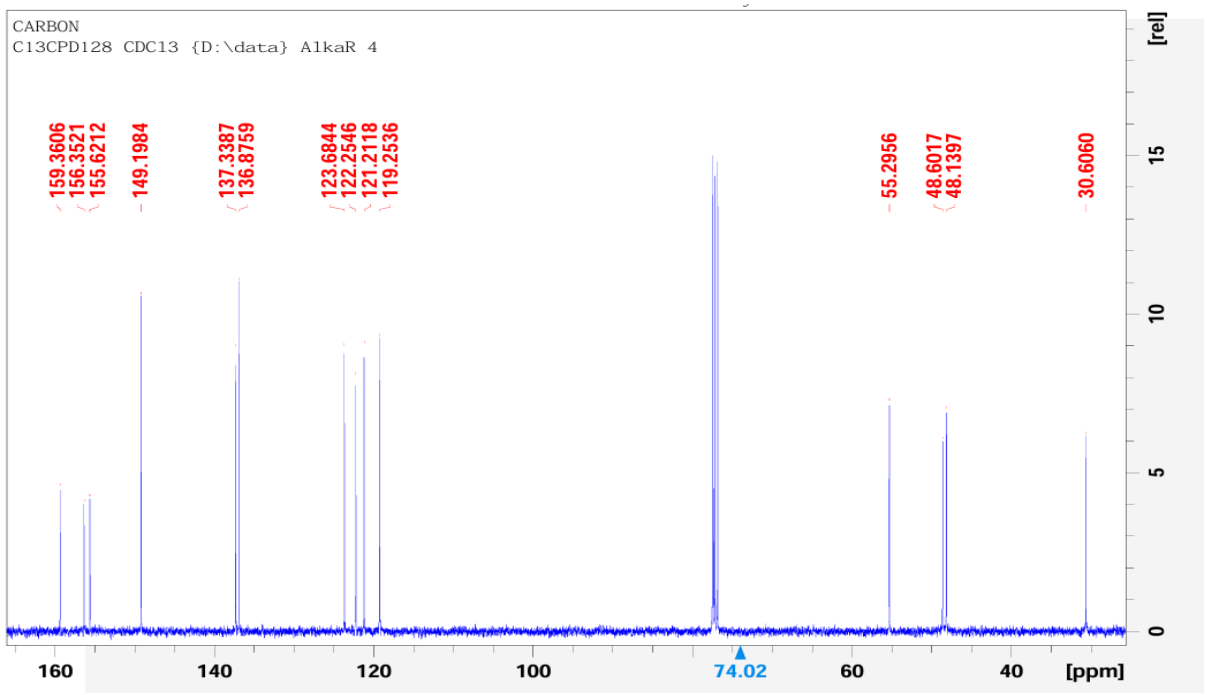

figure 37: The ^{13}C NMR spectrum of bmdpt in $CDCl_3$

figure 38: The Mass spectrum of bmdpt.

The bmdet ligand was converted to the hydrochloride salt by treatment with 1 M hydrochloric acid, and removal of this under reduced pressure gave a pale-yellow solid. The residue was then dissolved in ethanol and evaporated to dryness, and this process was repeated several times to ensure complete removal of residual HCl. The final product, bmdet·xHCl, was obtained as a pale-yellow solid, confirming successful conversion to the corresponding salt form.

In a similar manner, bmdpt was converted to bmdpt.xHCl, giving a pale-pink solid.

As we did not have access to microanalysis, the number x is unknown in both cases. However, it is assumed to be 3 for synthetic purposes.

3.2 Complex synthesis

Having prepared the two new ligands as the hydrochloride salts, it then made sense to utilise transition metal carbonates as the starting materials to prepare metal complexes of these.

Direct reactions between ligand hydrochloride salts and simple metal salts such as $[M(OH_2)_6]^{2+}$ are often unsuccessful because the metal ions must compete with protons for binding to the donor atoms of the ligand. In contrast, using metal carbonates provides a more effective approach. When carbonates react with protonated ligands, carbon dioxide and water are released, which generates

the neutral (free base) ligand directly in the reaction mixture. This allows the ligand to coordinate readily to the metal ion. This also overcomes any ligand solubility problems in water.

To access cobalt in the +3 oxidation state, the complex $Na_3[Co(O_2CO)_3].3H_2O$ was also used as a starting material. This compound is an uncommon example of a Co(III) complex coordinated exclusively by oxygen donor atoms. It is thermally unstable at room temperature and therefore must be stored at low temperatures. Upon reaction with ligand hydrochloride salts, one or more carbonate ligands are displaced depending on the extent of ligand protonation. This complex has been widely used as a precursor in the synthesis of Co(III) carbonate-based coordination compounds.

We are interested in cobalt complexes of the two newly developed ligands for several practical reasons. Cobalt commonly exists in two oxidation states, Co^{2+} and Co^{3+}, and these differ significantly in their chemical behaviour and ease of characterisation. Complexes containing Co^{2+} have a d^7 electronic configuration and are always paramagnetic. As a result, they contain unpaired electrons, which cause severe signal broadening in NMR spectra. This makes NMR analysis unreliable and difficult to interpret. In addition, Co^{2+} complexes are substitutionally labile, meaning that ligands can exchange rapidly in solution. This further complicates characterisation, particularly in solution studies. In contrast, Co^{3+} complexes usually have a low-spin d^6 electronic configuration and are therefore diamagnetic. This allows them to give sharp and well-defined NMR signals, making NMR spectroscopy a useful tool for confirming product formation. Although Co^{3+} complexes are often difficult to prepare directly due to their substitutional inertness, once formed they are generally very stable and resistant to ligand exchange. These properties make Co^{3+} complexes more suitable for reliable synthesis and characterisation. Complexes with other metal centres were also synthesised and analysed to compare the differences between various metal centres.

$[Co_2(Hbmdet)_2Cl_2](ClO_4)_6$

The cobalt complex of bmdet was synthesised by reacting the protonated ligand (assumed to be bmdet·3HCl) with the cobalt(III) carbonate precursor ($Na_3[Co(CO_3)_3].3H_2O$) in aqueous solution. Upon mixing, a colour change from green to red/orange was observed, indicating coordination of the bmdet ligand; Co(III) complexes having 6 N atoms coordinated to the metal ion are generally orange in colour. Gentle heating promoted the reaction, during which carbon dioxide was released

and the solution darkened, consistent with coordination of the ligand to the cobalt centre. After completion, the reaction mixture was filtered to remove insoluble material, and the filtrate was purified using cation-exchange (Dowex 50W-X2) chromatography. An initial minor impurity band was discarded, while the desired cobalt complex was eluted with 5 M HCl. Removal of solvent gave the complex as an orange solid. The dimeric nature of this complex was confirmed by X-ray crystallography (see below).

The mass spectrum of this complex shows a base peak at *m/z* = 249.0903 consistent with the formula $CoC_{26}H_{29}N_7^{2+}$ (calculated *m/z* =249.0900) and thus the formulation $[Co(bmdet)]^{2+}$, a mononuclear species containing one Co(II) ion and one bmdet ligand. This is at odds with the crystal structure of this complex and the m/z value is obviously much lower than the value expected for a dimeric $[Co_2(Hbmdet)_2Cl_2]^{n+}$ cation.. However, this observation can be rationalised by proposing that the dimeric complex breaks apart under the mass spectrometry conditions, and that the initial Co(III) ions reduce to Co(II). This is commonly observed in the mass spectra of Co(III) complexes that do not contain ionisable protons, loss of which helps to lower the charge on the complex.

figure 39: The mass spectrum of $[Co_2(Hbmdet)_2Cl_2](ClO_4)_6$.

Close examination of the mass spectrum in figure 39 shows a small peak at *m/z* = 496.1652. This is consistent with a complex having the formula $[CoC_{26}H_{27}N_7]^+$ - in other words, the mononuclear complex $[Co(bmdet\text{-}2H)]^+$. The peak spacing of *m/z* ~ 1 confirms this as having a 1+ charge. A small peak at m/z = 533.1497 is consistent with the formula $[CoC_{26}H_{29}N_7Cl]^+$ and corresponds to the mononuclear complex $[Co(bmdet)Cl]^+$; the isotope pattern is also consistent with the presence of Cl, and the peak spacing of m/z ~ 1 confirms the 1+ charge on the ion. These results show that formation of a mononuclear complex is possible, but unfortunately provide no information as to the mode of bonding of the heptadentate bmdet ligand.

The crystal structure of the complex (see below) shows that two Co(III) centres are coordinated by two bmdet ligands, leading to the formation of a dimeric complex. The complex cation possesses a mirror plane that passes through the two central nitrogen atoms, as well as a twofold rotational axis along the line connecting the two Co(III) metal centres. This molecular symmetry explains the presence of thirteen distinct signals in the ^{13}C NMR spectrum. Unfortunately, both the ^{1}H and ^{13}C NMR spectra of the complex were not optimal. The ^{1}H spectrum was extremely difficult to interpret. However, the observation of 13 peaks, 10 aromatic and 3 aliphatic, in the ^{13}C NMR spectrum is consistent with the presence of high symmetry in the dimeric cation. Due to time constraints, further purification of the complex using column chromatography could not be carried out, which could have led to better quality NMR data.

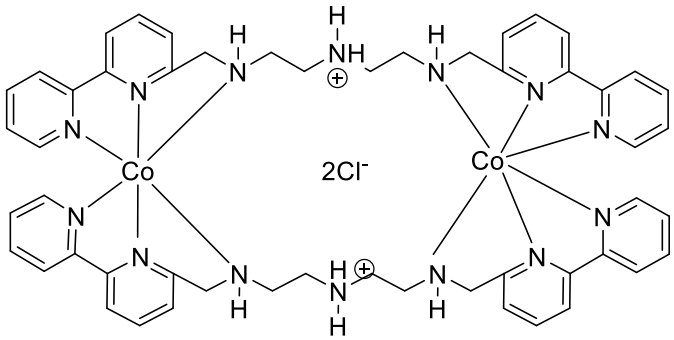

figure 40: The chemical structure of $[Co_2(Hbmdet)_2Cl_2](ClO_4)_6$.

Figure 40 shows the structure of the complex cation, while crystal data, and bond lengths and angles are given in Table 1. The structure of the cation comprises two bmdet ligands, two Co(III) ions, and two encapsulated Cl^- ions. While the cation is well ordered, there is disorder in the anions and solvent molecules which makes the exact formulation of the overall complex uncertain. This

is reflected in the rather high value of R_1 (6.81 %) and that fact that some atoms could not be sensibly assigned. As each bmdet ligand contains a protonable N atom, and the complex was isolated from strongly acidic solution on a cation exchange resin, it is assumed that both N atoms in the complex are protonated. Thus the cation can be formulated as $[Co_2(Hbmdet)_2Cl_2]^{6+}$, and views of its structure are shown in figure 41 and 42.

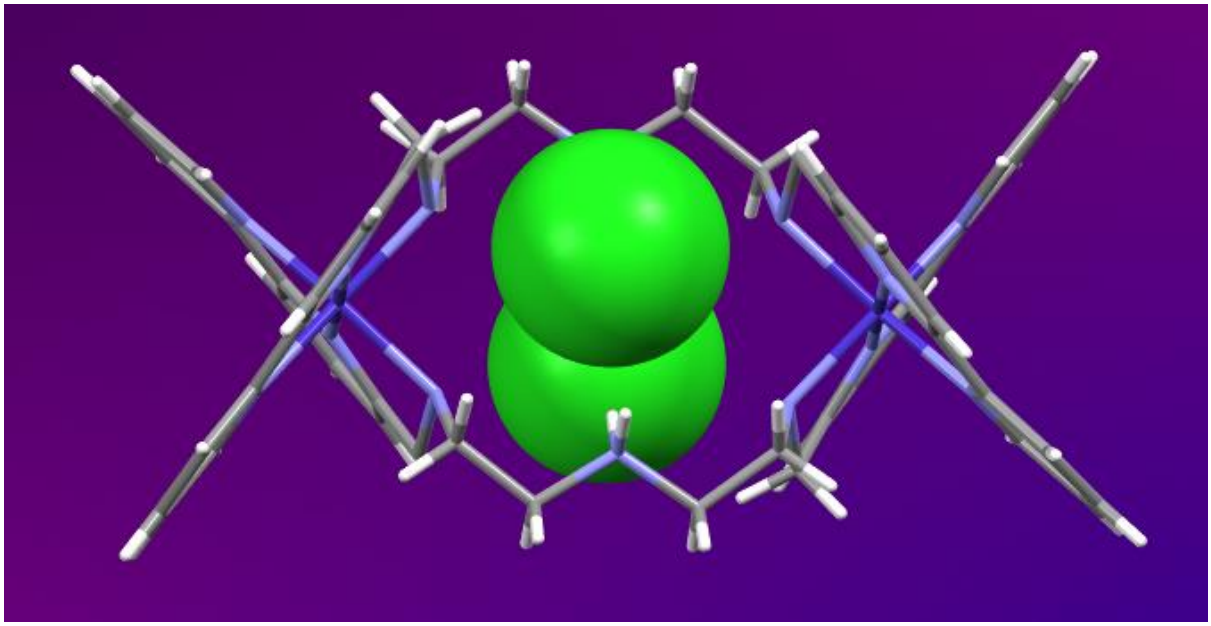

figure 41: The X-ray structure of $[Co_2(Hbmdet)_2Cl_2](ClO_4)_6$.

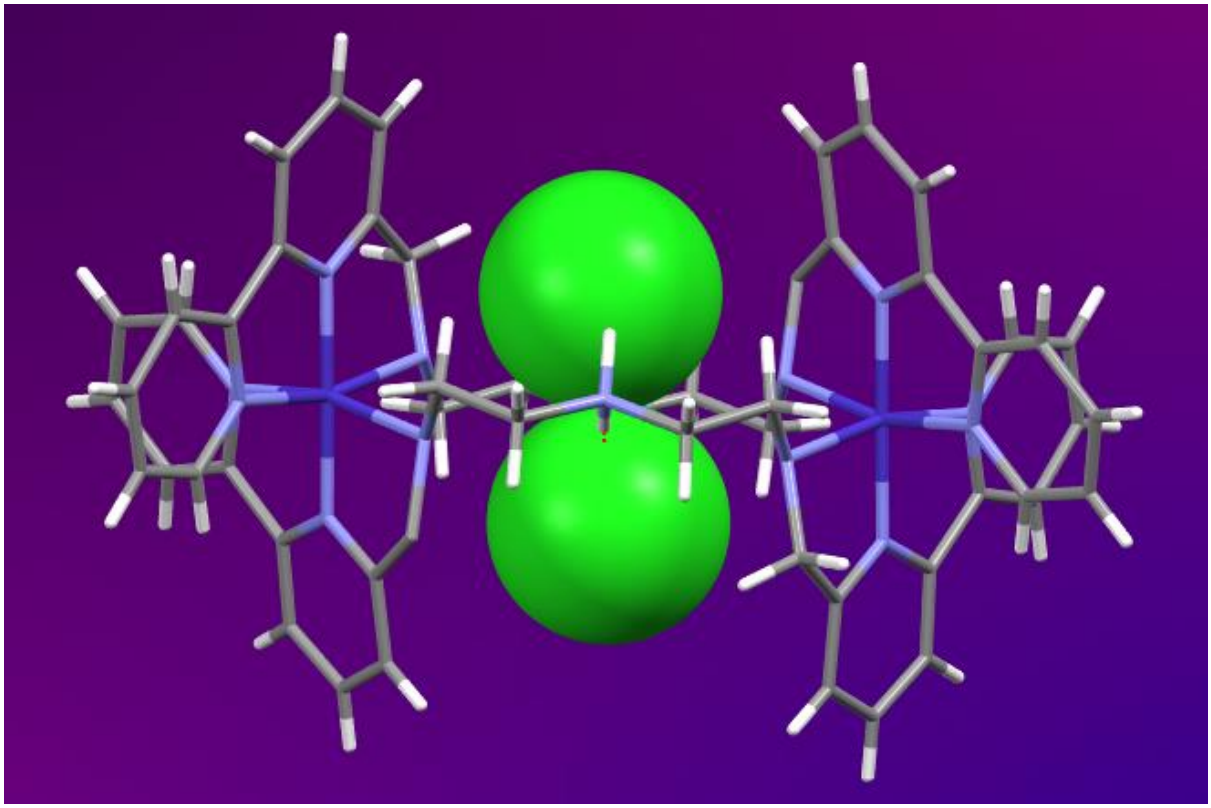

figure 42: The X-ray structure of $[Co_2(Hbmdet)_2Cl_2](ClO_4)_6$.

Table 1. Crystal data and structure refinement for $[Co_2(Hbmdet)_2Cl_2](ClO_4)_6$.

Identification code	shelx	
Empirical formula	C15.5 H18 Cl2 Co0.50 N3.50 O6	
Formula weight	449.54	
Temperature	100(2) K	
Wavelength	0.71073 Å	
Crystal system	Triclinic	
Space group	P-1	
Unit cell dimensions	a = 11.2229(6) Å	α= 74.763(3)°.
	b = 12.6196(7) Å	β= 69.938(3)°.
	c = 15.4699(8) Å	γ = 76.780(3)°.
Volume	1962.35(19) $Å^3$	
Z	4	
Density (calculated)	1.347 Mg/m^3	
Absorption coefficient	0.702 mm^{-1}	
F(000)	814	
Crystal size	0.1 x 0.05 x 0.02 mm^3	

Theta range for data collection	1.692 to 29.806°.
Index ranges	-14<=h<=14, -13<=k<=16, -19<=l<=20
Reflections collected	35673
Independent reflections	9259 [R(int) = 0.0767]
Completeness to theta = 25.242°	95.9 %
Refinement method	Full-matrix least-squares on F^2
Data / restraints / parameters	9259 / 0 / 525
Goodness-of-fit on F^2	1.063
Final R indices [I>2sigma(I)]	R1 = 0.0681, wR2 = 0.1872
R indices (all data)	R1 = 0.1192, wR2 = 0.2275
Extinction coefficient	n/a
Largest diff. peak and hole	1.408 and -1.163 e.$Å^{-3}$

Table 2: Bond lengths [Å] about the Co(III) ions for $[Co_2(Hbmdet)_2Cl_2](ClO_4)_6$.

Co(1)-N(21)	1.873(3)
Co(1)-N(8)	1.878(3)
Co(1)-N(15)	1.941(4)
Co(1)-N(17)	1.950(4)
Co(1)-N(13)	2.011(4)
Co(1)-N(20)	2.031(4)

Table 3: Bond angles [°] about the Co(III) ions for $[Co_2(Hbmdet)_2Cl_2](ClO_4)_6$.

N(21)-Co(1)-N(8)	178.67(18)
N(21)-Co(1)-N(15)	96.49(15)
N(8)-Co(1)-N(15)	82.28(16)
N(21)-Co(1)-N(17)	82.32(15)
N(8)-Co(1)-N(17)	98.25(14)
N(15)-Co(1)-N(17)	93.57(15)
N(21)-Co(1)-N(13)	82.47(14)
N(8)-Co(1)-N(13)	97.02(14)
N(15)-Co(1)-N(13)	91.27(15)
N(17)-Co(1)-N(13)	164.47(14)
N(21)-Co(1)-N(20)	98.95(15)
N(8)-Co(1)-N(20)	82.26(15)
N(15)-Co(1)-N(20)	164.50(14)
N(17)-Co(1)-N(20)	89.73(15)
N(13)-Co(1)-N(20)	89.51(15)

Each bmdet ligand in the complex cation binds to both Co(III) ions through two bipyridine N and one aliphatic N atoms in a meridional arrangement, making each Co(III) ion six-coordinate. One N aliphatic N atom, the central N atom of the trien residue, remains unbound in both ligands, and acts as part of the -$CH_2CH_2NCH_2CH_2$- bridge between the two Co(III) ions. The bipyridine moieties of each bmdet ligand are *cis* to each other in the complex cation, and as a result, each bmdet ligand, and hence the entire cation, is not helical. The Co-N bond lengths span an unusually large range from 1.873 Å to 2.031 Å, the former being extremely short and the latter being rather long for Co(III). The two shortest Co-N bonds, 1.873 Å and 1.878 Å, involve the non-terminal bipyridine N atom, and this has been seen previously in both the $[Co(bmet)]^{3+}$ and $[Co(bmpp)]^{3+}$ cations, where the analogous non-terminal Co-N bonds (1.8653 Å and 1.8636 Å in the former, and 1.8592 Å and 1.8621 Å in the latter) were ~ 0.08 Å shorter than any of the other Co-N bonds. The Co-N bonds involving the terminal bipyridine N atom are 1.941 Å and 1.950 Å, which are considered normal for Co(III)-N species. The longest Co-N bonds, 2.011 Å and 2.031 Å, involve the terminal N atom of the trien moiety, and are more comparable to the lengths of Co(II)-N bonds. Indeed, the mononuclear Co(II) complex of the ligand L shown in figure 43.

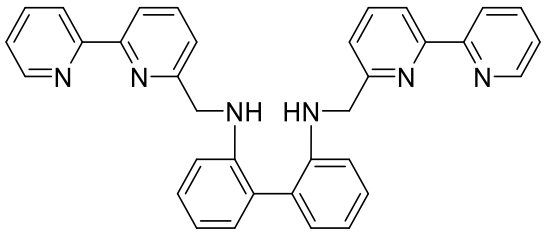

figure 43: The structure of ligand L.

has Co-N bond lengths of 1.985 Å, 1.989 Å, 2.095 Å, 2.117 Å, 2.188 Å, and 2.199 Å, with the shortest pair of bonds being those to the non-terminal bipyridine N atoms, and the longest pair to the aliphatic N atoms, similar to the trends found in the dimeric cation above.[41] *Cis* N-Co-N angles about the Co(III) ions in the $[Co_2(Hbmdet)_2Cl_2]^{6+}$ cation range from 82.26° to 98.95°, while the corresponding *trans* angles range from 164.47° to 178.67°, giving an approximately octahedral geometry about both Co ions. The bmdet ligands bind to the two Co(III) ions in such a way so as to form a 16-membered metallocyclic ring, which contains two Co(III) ions, six N atoms and eight C atoms. The approximate dimensions of this ring can be obtained from the Co-Co distance (8.281

Å) and the N-N distance between the central trien N atoms (5.300 Å). Given that these N atoms are protonated, and that each Co ion has a 3+ charge, such a sized ring should show high affinity for binding monoatomic anionic species. Indeed, the complex crystallises with a Cl^- ion bound in each of the two cavities formed by the 16-membered ring and the non-terminal pyridine rings of a bmdet ligand (the centroid-centroid distance of these pyridine rings is 8.148 Å and the angle between the pyridine ring planes is 73.59°). The Cl…Cl distance is 3.441 Å, which, for comparison, is within the range of the *cis*-Cl…Cl distances found in a number of Co(II) and Co(III) tetraamine complexes.[42–45] Similar situations are found in the solid state structures of the protonated free ligand [18]aneN_6, which comprises an 18-membered ring with 6 N atoms (figure 44).

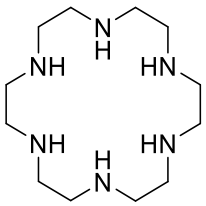

figure 44: The structure of the [18]N_6 ligand

The crystal structure of hexaprotonated (H_6[18]aneN_6)Cl_6.4H_2O shows one Cl^- ion bound on each side of the ring, with a Cl…Cl distance of 4.427 Å (figure 45).[46] Such binding of two Cl^- ions on either side of the ring is also observed in hexaprotonated (H_6[18]aneN_6)(HSO_4)$_2Cl_4$.2H_2O[46] (Cl…Cl = 4.209 Å), hexaprotonated (H_6[18]aneN_6)(NO_3)$_4Cl_2$.2H_2O[47] (Cl…Cl = 4.257 Å), and tetraprotonated (H_4[18]aneN_6)(NO_3)$_2Cl_2$.2H_2O[48] (Cl…Cl = 3.742 Å),. It is interesting to note that the Cl…Cl distance in the [Co_2(Hbmdet)$_2Cl_2$]$^{6+}$ cation is significantly less than the distances in these protonated ligands, given than all but one have the same 6+ charge. This suggests the important role of the pyridyl rings in forming a cooperative binding cleft above and below the 16-membered aliphatic ring.

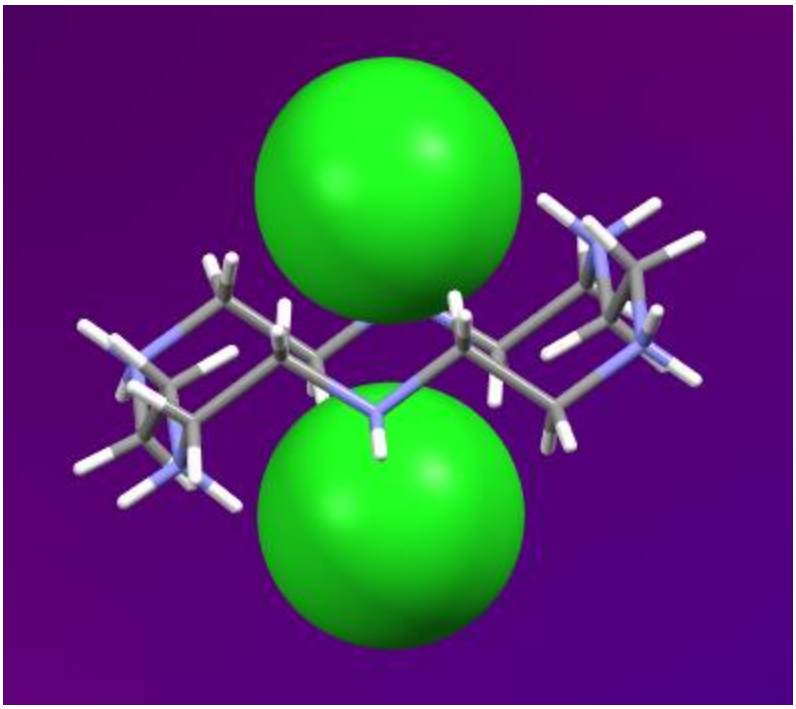

figure 45: The crystal structure of H_6[18]aneN_6)Cl_6.4H_2O Complex.

In addition, the orientation of the N-H protons appears to influence the strength of the Cl^- binding, owing to the different number of possible Cl…H hydrogen bonding interactions. In the $[Co_2(Hbmdet)_2Cl_2]^{6+}$ cation, all N-H protons are oriented such that they point to the interior of the aliphatic ring, making all Cl…N distances less than 4 Å (3.116 Å, 3.128 Å, 3.194 Å, 3.252 Å, 3.627 Å and 3.975 Å). In contrast, only 2 N-H protons in (H_6[18]aneN_6)$(NO_3)_4Cl_2$.2H_2O point inside the aliphatic ring owing to its greater flexibility, and the Cl…N distances involving these (3.086 Å and 3.244 Å) are much less than the others (4.577 Å, 3.953 Å, 4.720 Å and 4.735 Å).[47] The same arrangement of N-H protons is also observed in (H_6[18]aneN_6)Cl_6.4H_2O[46] and (H_6[18]aneN_6)$(HSO_4)_2Cl_4$.2H_2O,[46] giving 2 short and 4 long Cl…N distances, while tetraprotonated (H_4[18]aneN_6)$(NO_3)_2Cl_2$.2H_2O[48] has four N-H bonds pointing to the interior of the ring, resulting in all Cl…N distances being less than 4 Å (3.061 Å, 3.280 Å, 3.313 Å, 3.325 Å, 3.873 Å, and 3.962 Å) and a correspondingly short Cl…Cl distance of 3.742 Å.

$[Co_2(bmdpt)_2Cl](ClO_4)_5$

This cobalt complex of bmdet was synthesised by reacting the protonated ligand (assumed to be bmdet·3HCl) with the cobalt(III) carbonate precursor $Na_3[Co(CO_3)_3)$.3H_2O in aqueous solution,

resulting in a change of colour and gas evolution on mild heating. After removing insoluble material by filtration, the solution was purified using a cation-exchange column (Dowex 50W-X2). The desired product was collected on elution with 5 M HCl, and isolated as an orange solid after solvent removal. The large number of peaks in the mass spectrum suggest that the complex may not be pure.

The mass spectrum shows an intense peak at *m/z* = 262.0981 that is consistent with the doubly charged species $[CoC_{28}H_{31}N_7]^{2+}$ (calculated *m/z* = 262.0980, with the isotopomeric peak spacing being ~1/2). At first, this appears difficult to assign with confidence, as it apparently corresponds to the formula $[Co(bmdpt\text{-}2H)]^{2+}$ in which two protons have been lost from the ligand. This would then result in a 1+ charge on the overall complex, and appearance of a peak at twice the observed *m/z* value. Such a peak, while of relatively low intensity, is indeed seen at *m/z* = 524.1965, consistent with the singly charged species $[CoC_{28}H_{31}N_7]^{1+}$ (calculated *m/z* = 524.1970), implying the formula $[Co(bmdpt\text{-}2H)]^{+}$. However, it is most likely that in fact the peak arises from the presence of the half-reduced monoimine ligand pictured in figure 46.

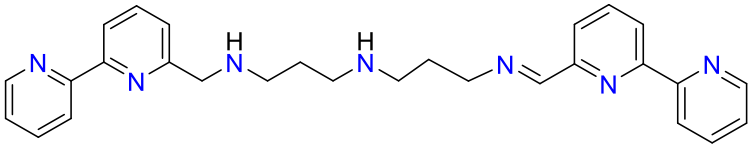

figure 46: The half-reduced monoimine ligand.

The Co complex of this would have a formula of $CoC_{28}H_{31}N_7$ and a charge of 3+. Monoreduction of the Co centre would result in the $[CoC_{28}H_{31}N_7]^{2+}$ species and this is chemically reasonable; there are many examples of Co(III) complexes undergoing reduction under mass spectrometry conditions. Hence the singly charged $[CoC_{28}H_{31}N_7]^{1+}$ species at *m/z* = 524.1965 could be either $[Co(bmdpt\text{-}2H)]^{+}$ or the direduced monoimine complex. The moderately intense signal at *m/z* = 262.6021 is however, consistent with the doubly charged species $[CoC_{28}H_{32}N_7]^{2+}$ and the formula $[Co(bmdpt\text{-}H)]^{2+}$, in which only one proton has been lost from the ligand, and the resulting 2+ charge makes chemical sense. The remaining intense peaks in the spectrum cannot be assigned to any obvious species containing the bmdpt ligand, and it may be that they derive from residues of samples previously analysed in the mass spectrometer.

The NMR spectrum was also not obvious and didn't justify the formation of a pure complex. Further purification of the complex was required, which was not possible due to time constraints.

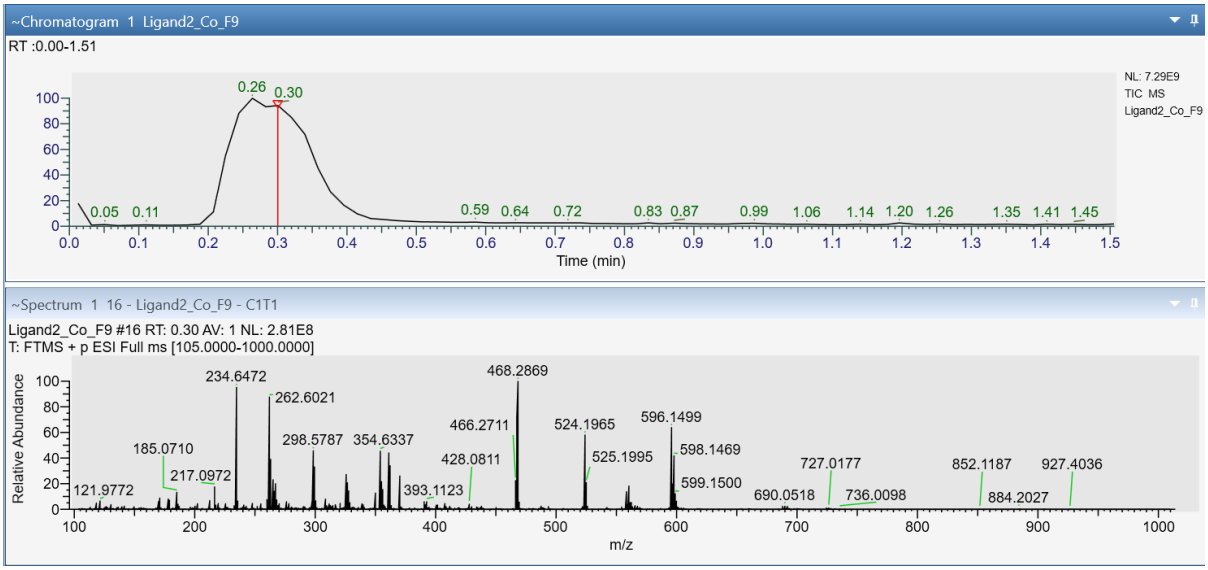

figure 47: The Mass spectrum of $[Co_2(Hbmdpt)_2Cl_2](ClO_4)_6$.

3.3 Mass spectral studies of transition metal complexes of bmdet and bmdpt

Despite numerous attempts at crystallising transition metal complexes of the bmdet and bmdpt ligands, no X-ray quality crystals were obtained using a variety of solvents and counterions. Therefore, it was decided to investigate these reactions by mass spectrometry, in the hope of seeing evidence for the formation of multinuclear species of the types seen for the bmot and bmpt ligands discussed in Chapter 1. Perchlorate and acetate salts of the transition metals were reacted with varying amounts of the heptadentate ligand in either acetonitrile or methanol. This section gives the results of these investigations.

Cu^{2+} + bmdet

Reaction of $[Cu(OH_2)_6](ClO_4)_2$ with bmdet in MeOH at the mole ratio 0.5:1 gave a base peak at m/z = 251.0886, which corresponds to the formula $[Cu(bmdet)]^{2+}$ (calculated m/z = 251.0880). The presence of Cu was confirmed by the appearance of an isotopomeric signal at 252.0876 approximately one-third the intensity of the base peak, due to the ^{65}Cu isotope. Another relatively intense peak (60 %) appeared at m/z = 334.1151. The isotope pattern associated with this peak is consistent with the presence of Cu, and the peak spacing is consistent with a 2+ species. A formula

that fits this is $[CuC_{37}H_{35}N_9]^{2+}$ (calculated *m/z* = 334.1150), and this can be rationalised by proposing the peak to derive from a Cu^{2+} complex of the ligand $C_{37}H_{35}N_9$ (L_1) shown in figure 48.

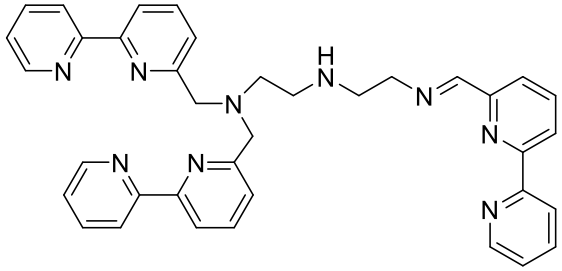

figure 48: The Structure of the L_1 ligand

It is plausible that this could be formed during the synthesis of bmdet through overreaction of one of the primary amines of diethylenetriamine with 2,2'-bipyridine-6-carbaldehyde, and then incomplete reduction of the imine. Indeed, the mass spectrum of bmdet does show a low intensity (~8 %) peak at *m/z* = 606.3085, corresponding to the formula $[C_{37}H_{36}N_9]^+$, and thus this appears to be a chemically reasonable assignment of the *m/z* = 334.1151 peak.

A similar spectrum is observed at a mole ratio of 1:1, but at 2:1 and 3:1, the peak due to $[Cu(bmdet)]^{2+}$ all but disappears and the *m/z* = 334.1151 $[CuL_1]^{2+}$ peak becomes the base peak.

Similar behaviour is observed when $Cu(OAc)_2.H_2O$ is used as the starting material at the 0.5:1 mole ratio, but at 1:1 and 2:1 mole ratios, a peak at *m/z* = 330.6175 becomes the base peak. This looks to be due to a 2+ ion, and the isotope pattern is consistent with the absence of Cu. The 3:1 mole ratio gives the *m/z* = 334.1151 $[CuL_1]^{2+}$ peak again as the base peak.

Mn^{2+} + bmdet

Reaction of $[Mn(OH_2)_6](ClO_4)_2$ with bmdet in MeOH at the mole ratio 0.5:1 gave a base peak at *m/z* = 220.6315, and a slightly less intense (80 %) peak at *m/z* = 330.1192. Neither of these correspond to the expected $[Mn(bmdet)]^{2+}$ ion (calculated *m/z* = 247.0930), which appears as a low intensity (10 %) peak at *m/z* = 247.0927. The peak spacing of 0.5 associated with this confirms it being a 2+ ion. As Mn has only a single stable isotope (^{55}Mn), the isotope patterns are of little use in confirming assignments. The base peak at *m/z* = 220.6315 corresponds to the diprotonated free ligand $[C_{26}H_{31}N_7]^{2+}$ (calculated *m/z* = 220.6310), suggesting that Mn^{2+} has little affinity for the free ligand, while a tiny (< 5 %) peak corresponding to the monoprotonated free ligand is

observed at *m/z* = 440.2555 (calculated *m/z* = 440.2560). The peak at *m/z* = 330.1192 is due to a 2+ ion, and the species giving rise to this does not contain chlorine. This looks to be due to the complex $[MnL_1]^{2+}$ (calculated *m/z* = 330.1190). As the metal to ligand ratio increases, the spectra look quite different. At the 1:1 ratio a peak at *m/z* = 331.6179 becomes the base peak, to the near exclusion of any other peaks, while at 2:1 and 3:1 ratios, the peaks at *m/z* = 220.6315 and *m/z* = 330.1192 again predominate.

When $Mn(OAc)_2.4H_2O$ is used as the starting material, no peak due to the free ligand is observed, and the $[Mn(bmdet)]^{2+}$ peak at *m/z* = 247.0927 is the base peak at all metal to ligand ratios. A low intensity (~10-20%) peak at 553.1995 is observed at all mole ratios; this is consistent with the formula $[MnC_{28}H_{32}N_7O_2]^+$ and the formulation $[Mn(bmdet)(OAc)]^+$.

figure 49: The Mass spectrum of $[Mn(bmdet)](ClO_4)_2$.

Fe^{2+} + bmdet

Reaction of $[Fe(OH_2)_6](ClO_4)_2$ with bmdet in MeOH at the mole ratio 0.5:1 gave a base peak at *m/z* = 247.5910, and a much less intense (20 %) peak at *m/z* = 330.6177. The former corresponds to a formula of $[FeC_{26}H_{29}N_7]^{2+}$ and hence the complex $[Fe(bmdet)]^{2+}$ (calculated *m/z* = 246.5911). The isotope pattern for Fe can be somewhat indistinct, with peaks deriving from the most abundant (^{56}Fe, ~92 %) and second-most abundant (^{54}Fe, ~ 6%) isotopes being most obvious in the spectra of Fe complexes. In this case, the appropriate isotope pattern was observed. The peak at *m/z* =

330.6177 is consistent with the formula [$FeC_{37}H_{35}N_9$], and hence the complex $[FeL_1]^{2+}$ (calculated *m/z* = 330.6180). At metal to ligand ratios of 1:1, 2:1 and 3:1, the relative abundances of the *m/z* = 247.5910 and *m/z* = 330.6177 peaks remains the same, and a small peak due to the diprotonated free ligand is also observed.

figure 50: The Mass spectrum of $[Fe(bmdet)](ClO_4)_2$.

Co^{2+} + bmdet

Reaction of $[Co(OH_2)_6](ClO_4)_2$ with bmdet in MeOH at the mole ratio 0.5:1 gave a base peak at *m/z* = 249.0903, and a much less intense (10 %) peak at *m/z* = 332.1169. The former is consistent with the formula $[CoC_{26}H_{29}N_7]^{2+}$ and hence the complex $[Co(bmdet)]^{2+}$ (calculated *m/z* = 249.0900). The latter is consistent with the formula $[CoC_{37}H_{35}N_9]^{2+}$ and is likely the complex $[CoL_1]^{2+}$ (calculated *m/z* = 332.1170). The relative intensities of these peaks remain similar as the metal to ligand ratio increases from 0.5:1 to 1:1, 2:1 and 3:1. In addition, a small (~10 %) peak at *m/z* = 597.1297 is observed in all spectra. This is consistent with the formula $[CoC_{26}H_{29}N_7ClO_4]^{+}$ and hence the complex $[Co(bmdet)ClO_4]^{+}$ (calculated *m/z* = 597.1300).

Similar spectra are observed when $[Co(OAc)_2].4H_2O$ was used as a starting material, except that the peak at 597.1297 disappears (there is no perchlorate in the reaction mixture) and instead a peak

at *m/z* = 497.1735 (~20-30%) is observed. This corresponds to the formula $[Co(bmdet-H)]^+$ (calculated *m/z* = 497.1730).

Ni^{2+} + bmdet

Reaction of $[Ni(OH_2)_6](ClO_4)_2$ with bmdet in MeOH at the mole ratio 0.5:1 gave a base peak at *m/z* = 248.5914, and a much less intense (15 %) peak at *m/z* = 331.6179. The former is consistent with the formula $[NiC_{26}H_{29}N_7]^{2+}$ and hence the complex $[Ni(bmdet)]^{2+}$ (calculated *m/z* = 249.0900), while the latter is most likely due to $[NiL_1]^{2+}$ (calculated *m/z* = 331.6180). The spectra remain mostly unchanged as the mole ratio is increased, but a peak at *m/z* = 334.6149 appears at mole ratios of 1:1 and 1:2. The isotope pattern for this peak looks very much like that expected for a species containing Zn, and it is therefore suspected that this arises from the Zn + bmdet experiment which was run prior. A very low intensity (~8 %) peak at *m/z* = 596.1315 is observed in all spectra, consistent with the formula $[NiC_{26}H_{29}N_7]^{2+}$ and therefore the complex $[Ni(bmdet)ClO_4]^+$ (calculated *m/z* = 596.1320).

Zn^{2+} + bmdet

Reaction of $[Zn(OH_2)_6](ClO_4)_2$ with bmdet in MeOH at the mole ratio 0.5:1 gave a base peak at *m/z* = 251.5883, and a less intense (80 %) peak at *m/z* = 334.6149. The peak at *m/z* = 251.5883 is consistent with a complex cation having the formula $ZnC_{26}H_{29}N_7^{2+}$ (calculated *m/z* = 251.5880) and displays an isotope pattern consistent with the presence of a zinc atom. The peak at *m/z* = 334.6149 derives from a 2+ species and also contains a Zn atom. This is consistent with the formula $[ZnC_{37}H_{35}N_9]^{2+}$ and hence the complex $[ZnL_1]^{2+}$ (calculated *m/z* = 334.6150). The spectra remain essentially unchanged as the metal to ligand mole ratio increases from 0.5:1 to 1:1, 2:1, and 3:1.

figure 51: The Mass spectrum of $[Zn(bmdet)](ClO_4)_2$.

Co^{2+} + bmdpt

Reaction of $[Co(OH_2)_6](ClO_4)_2$ with bmdpt in CH_3CN at the mole ratio 1:1 gave a base peak at *m/z* = 171.0917, and a less intense (40 %) peak at *m/z* = 262.0981. The former is consistent with the formula $[C_{11}H_{11}N_2]^{1+}$, which corresponds to protonated 6-methyl-2,2'-bipyridine (calculated *m/z* = 171.0920), presumably formed by fragmentation of the bmdpt ligand. The latter is consistent with the formula $[CoC_{28}H_{31}N_7]^{2+}$ and is likely the complex $[Co(bmdpt\text{-}2H)]^{2+}$ (calculated *m/z* = 262.0980). The relative intensities of these peaks remain similar as the metal to ligand ratio increases from 1:1 to 2:1 and 3:1. In addition, a small (~10 %) peak at *m/z* = 336.0623 (a +1 species) is observed in all spectra, which cannot be sensibly assigned.

Cu^{2+} + bmdpt

Reaction of $[Cu(OH_2)_6](ClO_4)_2$ with bmdet in CH_3CN at the mole ratio 1:1 gave a base peak at *m/z* = 171.0917, which again corresponds to protonated 6-methyl-2,2'-bipyridine (calculated *m/z* = 171.0920). A less intense (40 %) peak at *m/z* = 265.1042 is consistent with the formula $[CuC_{28}H_{33}N_7]^{2+}$ and is likely the complex $[Cu(bmdpt)]^{2+}$ (calculated *m/z* = 265.1040). The presence of Cu was confirmed by the appearance of an isotopomeric signal at *m/z* = 255.6058 approximately one-third the intensity of the main peak, due to the ^{65}Cu isotope, and the peak spacing is consistent with a 2+ species. At the mole ratio of 2:1, a 1+ peak at *m/z* = 233.0135 that contains copper becomes the base peak; this corresponds to the formula $[CuC_{11}H_{10}N_2]^{+}$ and is

consistent with the Cu(I) complex [Cu(6-methyl-2,2'bipyridine)]$^+$. A moderate (25%) intensity 1+ peak at *m*/*z* = 403.0977 that contains copper is also observed; this corresponds to the formula $[CuC_{22}H_{20}N_4]^+$, and is most likely the Cu(I) complex [Cu(6-methyl-2,2'bipyridine)$_2$]$^+$. At the 3:1 mole ratio, a copper-containing 1+ peak at *m*/*z* = 144.9821 becomes the base peak. This corresponds to the formula $[CuC_4H_6N_2]^+$ (calculated *m*/*z* = 144.9821) It is difficult to propose a chemically reasonable structure for this species; the formula $C_4H_6N_2$ corresponds to 2-methyl and 4-methylimidazole, 3-methyl and 4-methylpyrazole, and a number of isomeric dihydropyrimidines, but it is hard to see how any of these molecules can be formed from the decomposition of bmdpt.

When Cu(OAc)$_2$.H$_2$O is used as the starting material at the 1:1 mole ratio, the peak at *m*/*z* = 171.0917 corresponding to protonated 6-methyl-2,2'-bipyridine becomes the base peak. A further intense (75%) peak at *m*/*z* = 185.0710 is consistent with the formula $[C_{12}H_{13}N_2]^+$ and appears to correspond, surprisingly, to protonated 6,6'-dimethyl-2,2'-bipyridine. It is difficult to determine the source of this; the clean NMR spectra of the ligand argue against it being a ligand impurity, and it is hard to envisage a decomposition pathway of the bmdpt ligand that would lead to this compound. The 2:1 and 3:1 mole ratio spectra are dominated by the *m*/*z* = 185.0709 peak and a 1+ copper-containing peak at *m*/*z* = 431.0562; the latter was thought to be [Cu(6,6'-dimethyl-2,2'-bipyridine)$_2$]$^+$ by analogy with the discussion above, but the very poor fit (calculated *m*/*z* = 431.1290) argues against this.

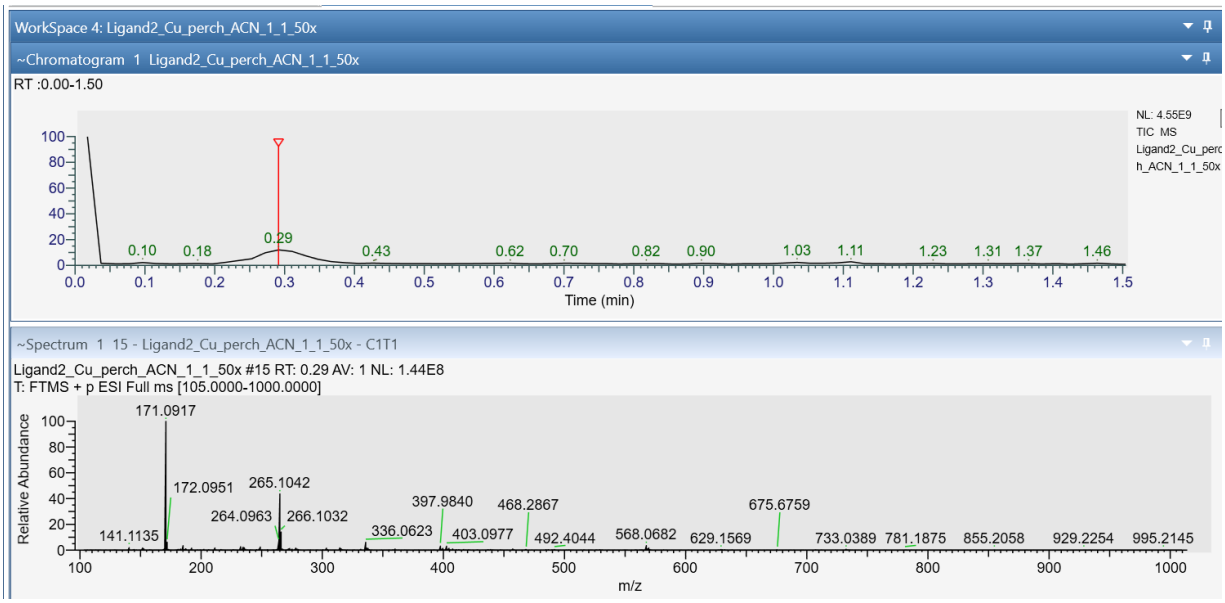

figure 52: The Mass spectrum of $[Cu(bmdpt)](ClO_4)_2$.

Fe^{2+} + bmdpt

Reaction of $[Fe(OH_2)_6](ClO_4)_2$ with bmdet in CH_3CN at the mole ratio 1:1 gives a base peak at *m/z* = 171.0917, again corresponding to protonated 6-methyl-2,2'-bipyridine (calculated *m/z* = 171.0920). A much less intense (20 %) peak at *m/z* = 261.6068 corresponds to a formula of $[FeC_{28}H_{33}N_7]^{2+}$ and hence the complex $[Fe(bmdpt)]^{2+}$ (calculated *m/z* = 261.6070). At the metal to ligand ratio of 2:1 the base peak remains same, but a 2+ peak with relative abundance ~80% is observed at *m/z* = 265.6039, which does not exhibit the isotope patterns for Fe. It appears that this is in fact due to $[Zn(bmdpt)]^{2+}$, which may have contaminated the sample from a prior run. At a 3:1 ratio, *m/z* = 171.0917 again becomes the base peak, to the near complete exclusion of all others. Little difference is observed when $[Fe(OAc)_2.4H_2O]$ is used as the starting material; the base peak in all cases is due to 6-methyl-2,2'-bipyridine and contamination by Zn^{2+} again appears to have occurred.

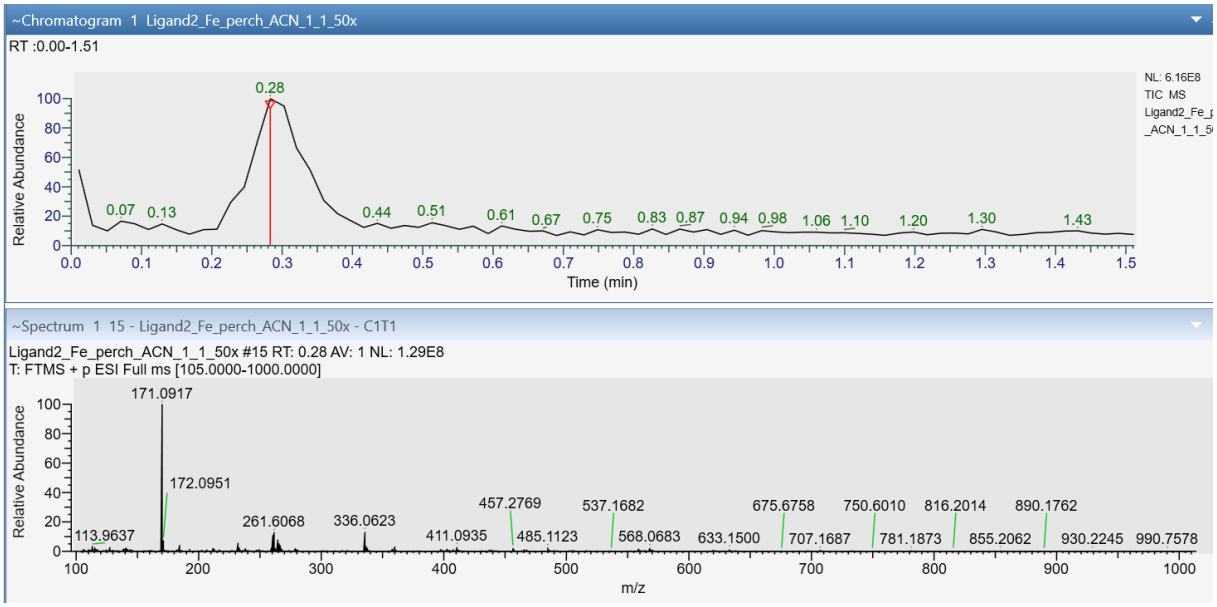

figure 53: The Mass spectrum of $[Fe(bmdpt)](ClO_4)_2$.

Mn^{2+} + bmdpt

Reaction of $[Mn(OH_2)_6](ClO_4)_2$ with bmdet in MeOH at the mole ratio 1:1 gave a base peak at *m/z* = 260.1005, and a less intense (50 %) peak at *m/z* = 265.1041. The former is consistent with the formula $[MnC_{28}H_{31}N_7]^{2+}$ (calculated *m/z* = 260.1010) and at first glance this corresponds to $[Mn(bmdpt\text{-}2H]^{2+}$, with the peak spacing of 0.5 confirms it being a 2+ ion. However, chemically this doesn't make sense, as loss of two protons from $[Mn(bmdpt)]^{2+}$ will result in the neutral [Mn(bmdpt-2H)] complex. This could be reconciled by proposing oxidation of Mn(II) to Mn(IV) but this would be extremely unlikely. The peak at *m/z* = 265.1041 appears due to $[Cu(bmdpt)]^{2+}$, a contaminant from a previous injection. As the metal to ligand ratio increases, the intensity of the contaminant peak increases to the point where it becomes the base peak, to the near exclusion of all others.

When $Mn(OAc)_2.4H_2O$ is used as the starting material the peak at *m/z* = 260.1005 predominates at all three mole ratios, and the Cu impurity peak is also observed.

Ni^{2+} + bmdpt

Reaction of $[Ni(OH_2)_6](ClO_4)_2$ with bmdet in MeOH at a 1:1 mole ratio gave a base peak at *m/z* = 360.3236, which does not contain nickel. It is consistent with the formula $[C_{22}H_{40}N_4]^+$ (calculated *m/z* = 360.3248) but a chemically reasonable assignment as either a derivative or fragment of the

bmdpt ligand cannot be made. A moderately intense peak (~50%) at *m*/*z* = 261.5992 is consistent with the formula $[NiC_{28}H_{31}N_7]^{2+}$ and the formulation $[Ni(bmdpt\text{-}2H]^{2+}$ (calculated *m*/*z* = 261.5990). However, as seen above, loss of two protons from $[Ni(bmdpt]^{2+}$ will result in a neutral molecule, which is chemically unreasonable. As the mole ratio increases from 1:1 to 2:1 and 3:1, the *m*/*z* = 360.3236 continues to predominate.

Interestingly, the situation is very different when MeCN is used as the solvent. Here, at the 1:1 mole ratio, the base peak at *m/z* = 171.9017 is protonated 6-methyl-2,2'-bipyridine (calculated *m/z* = 171.0920), while an intense (~90%) peak at *m/z* = 262.6070 is consistent with the formula $[NiC_{28}H_{33}N_7]^{2+}$, and corresponds to the complex $[Ni(bmdpt)]^{2+}$, in which the bmdpt ligand is formally neutral. At higher mole ratios, the spectra were very noisy, precluding assignment of any peaks.

Zn^{2+} + bmdpt

The reaction of $[Zn(OH_2)_6](ClO_4)_2$ with bmdet in MeOH at a 1:1 mole ratio gave a base peak at m/z = 265.6039, consistent with a complex cation of formula $[ZnC_{28}H_{33}N_7]^{2+}$ (calculated m/z = 265.6040) and displaying an isotope pattern consistent with the presence of a zinc atom. This peak predominates at the higher metal-to-ligand mole ratios, to the near total exclusion of all others. Very similar spectra are observed in MeCN as solvent, with the appearance of a moderate intensity (40%) peak due to protonated 6-methyl-2,2'-bipyridine.

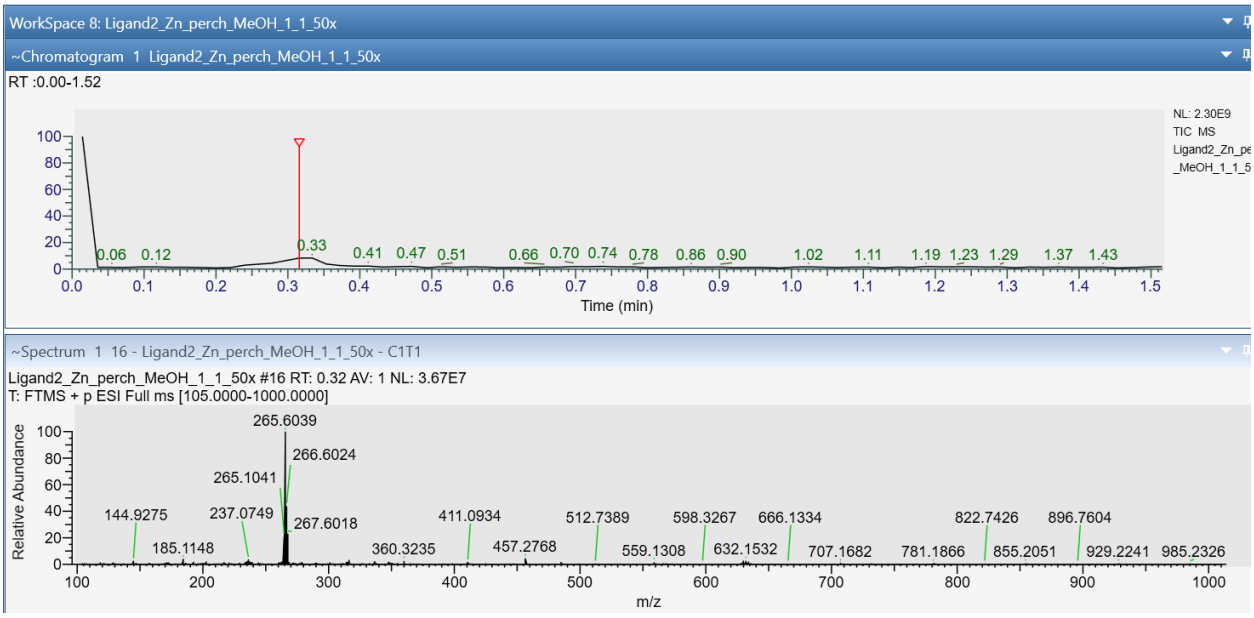

figure 54: The Mass spectrum of [Zn(bmdpt)]$(ClO_4)_2$.

3.4 Job Plots

A Job plot, also known as the method of continuous variation or Job's method, is an analytical technique that can be used to determine the stoichiometry of a reaction between a transition metal ion and a ligand. It is named after Paul Job who first reported the method in 1928.[49] By preparing solutions in which the mole fraction of metal and ligand vary while maintaining a constant total concentration and measuring the maximum absorbance of these, the composition of the predominant species in solution can be inferred from the maximum of the Job's plot.[50] This method has become widely used in many areas of chemistry, especially for determining the composition of complexes in solution.[51–53]

Job's method is based on the binding potential of one species (A) to another species (B) when those two species are present in a solution and is used to determine the ratio in which A and B bind.

To obtain a Job plot, aliquots of two equimolar stock solutions of metal and ligand are mixed in varying volumes such that the sum of the molar concentrations of the resulting solutions remain constant, while the metal-ligand ratio varies in each solution. UV/vis absorbance measurements of the prepared solutions are obtained and plotted against the mole fractions of the two species. The

stoichiometry of the reaction is determined from the maximum of the curve, which corresponds to the maximal formation of the complex. The peak of the plot correlates to the mole fraction of the ligands bound to a metal ion.

There are two main conditions that must be met to obtain a successful Job plot. Firstly, the system must conform to Beer's law, and secondly, there can only be one predominant complex species in solution under the experimental conditions. For instance, in the example above, the 1:1 complex predominates and there are not significant amounts of other species having different stoichiometries present.[54]

The stability of the complex formed is related to the curvature of the plotted lines. Complexes having higher formation constants afford straighter lateral segments of the curve allowing for easier determination of the position of the maximum. Two straight lines can easily be fitted, one with a positive slope due to the increase in the proportion of the complex, and the other with a negative slope due to its decreasing concentration as the stoichiometric point is exceeded. Complexes having relatively small formation constants result in more rounded plotted curves, and this can lead to more unreliable results. In this case, straight lines are plotted using the data points that are most distant from the maximum and the point at which these intersect determines the stoichiometry.[50,52,55]

The Job plots obtained from the reaction of Cu^{2+} with the ligands bmdet and bmdpt in CH_3CN are shown in figures 55 and 56. In both cases, the absorbance maximum lies at a mole fraction of ~ 0.4, suggesting a metal to ligand ratio of 2:3 for the predominant species in solution. This could be a dinuclear complex in which three ligands are wrapped around the two copper ions in a helical fashion.

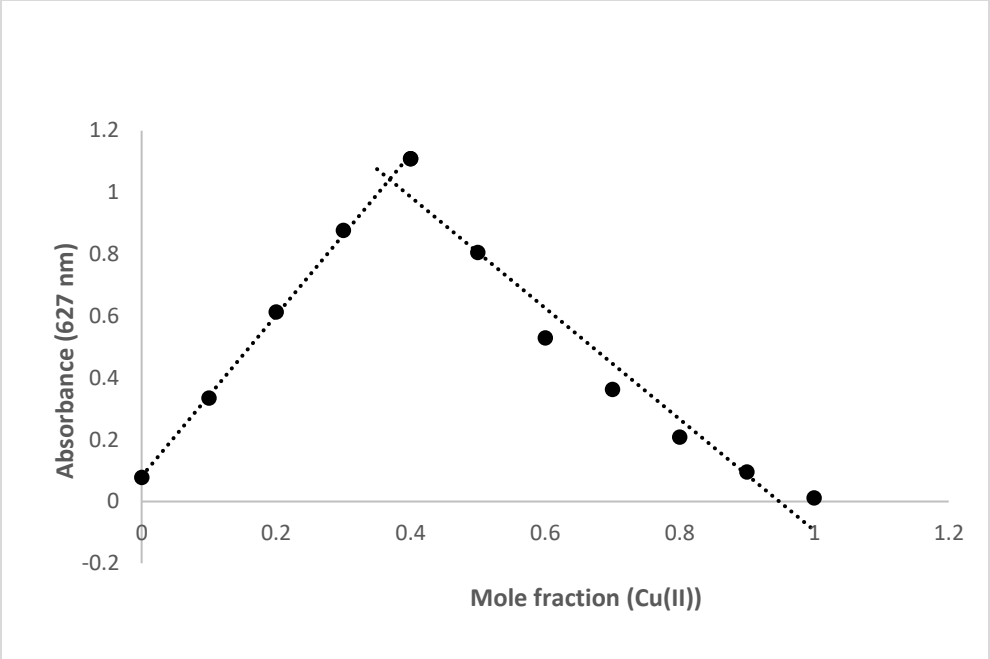

figure 55: The Job plot for the reaction between Cu^{2+} ions and the bmdet ligand.

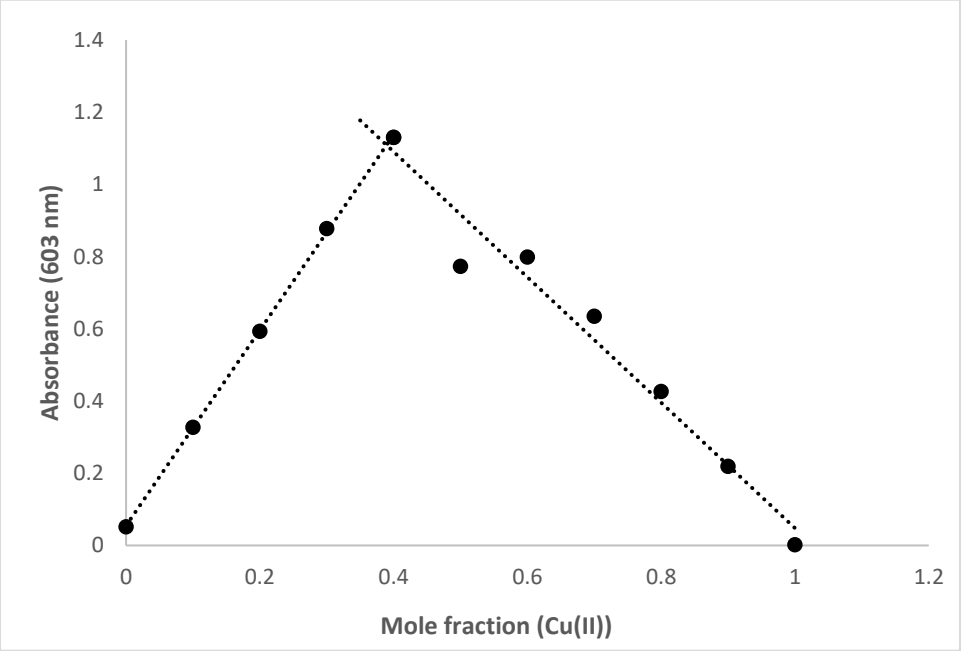

figure 56: The Job plot for the reaction between Cu^{2+} ions and the bmdpt ligand.

Figures 57 and 58 show the Job plots obtained for solutions of Co^{2+} with the ligands bmdet and bmdpt, in CH_3CN respectively. The two plots show a maximum absorbance at a mole fraction of

0.5, indicating that Co^{2+} has a binding stoichiometry of 1:1 with both ligands in solution, and the predominant complex formed in solution is $[M(L)]^{n+}$ in each case.

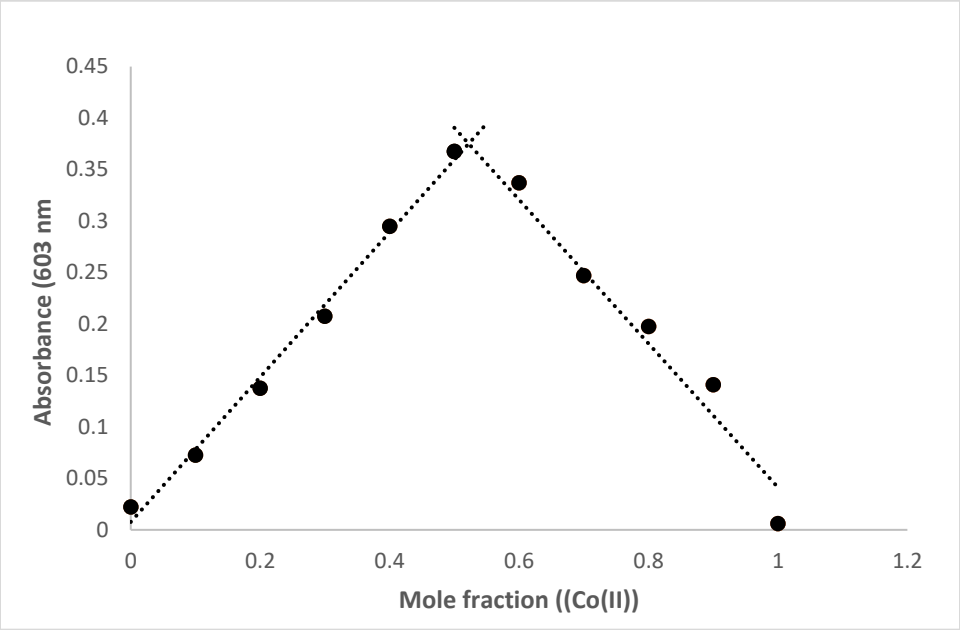

figure 57: The Job plot for the reaction between Co^{2+} and the bmdet ligand.

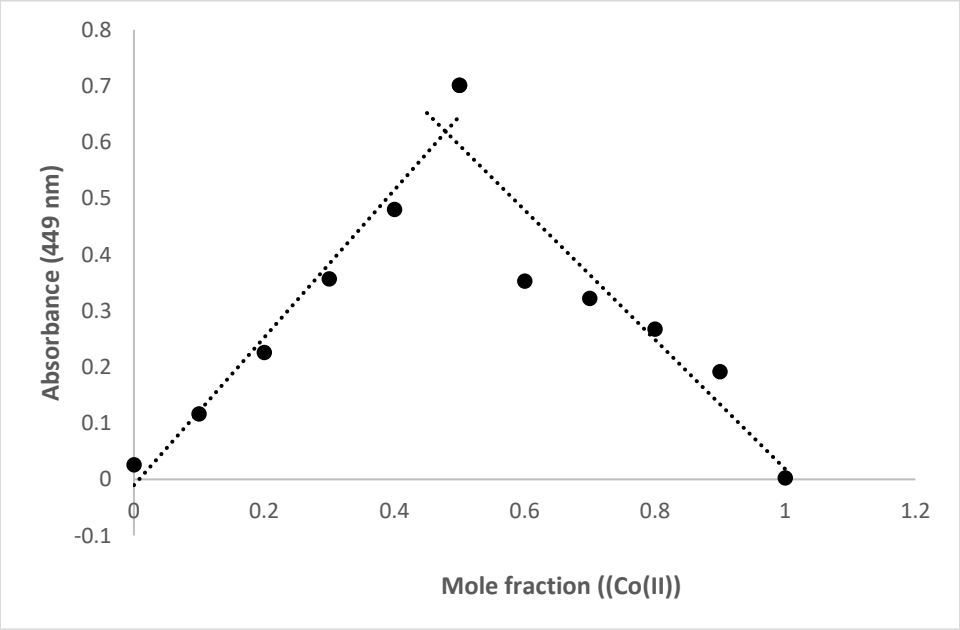

figure 58: The Job plot for the reaction between Co^{2+} and the bmdpt ligand.

4. Conclusions and Future Work

The aim of this thesis was to investigate the coordination of heptadentate N_7 ligands to first row transition metal ions. It was thought that these metal ions would be too small to be able to accommodate seven donor atoms and that they would then have to adopt some type of alternative binding geometry. Two novel heptadentate bipyridine-based ligands, bmdet and bmdpt, were prepared and characterised, and their reactions with a variety of first row transition metals were studied. The X-ray crystal structure of the complex $[Co_2(Hbmdet)_2Cl_2](ClO_4)_6$ showed that formation of a dimeric complex was preferred over monodentate coordination, with the two 6-coordinate Co(III) ions being bridged by two bmdet ligands, and one secondary N atom from each ligand being protonated and remaining uncoordinated. Interestingly, the complex geometry resulted in formation of two binding pockets which were occupied by two chloride anions, a process undoubtedly aided by the high charge (8+) on the cation.

Mass spectrometric studies of complexes formed with various first-row transition metals (Cu, Mn, Fe, Co, Ni, Zn) showed predominantly mononuclear species in solution. The absence of clear multinuclear species such as dimers or trimers in the mass spectra contrasts with the isolated solid-state dimeric cobalt complex. Job plot analyses further supported differing stoichiometries depending on the metal and ligand, with Cu(II) complexes suggesting possible multinuclear assemblies, while Co(II) favoured mononuclear 1:1 complexes.

The discrepancy between the solid-state crystallographic evidence of dimer formation and the mass spectrometric data lacking multinuclear species may be attributed to the fragmentation or dissociation of multinuclear complexes under the ionization conditions of mass spectrometry. Such processes are well-known and can lead to the predominance of mononuclear ions in the gas phase, masking the presence of multinuclear species in solution. Additionally, the dynamic equilibria of these complexes in solution may favour mononuclear species or rapid interconversion, further complicating detection of multinuclear assemblies by mass spectrometry.

In addition to the time constraints which are always present, challenges encountered during this work include difficulties in obtaining X-ray quality crystals for many complexes and complexities in interpreting NMR spectra due to paramagnetism or sample purity. If repeating this study, alternative synthetic strategies or crystallization conditions could be explored to improve crystal

growth, and complementary techniques such as EPR or advanced spectroscopies could be employed to better characterize solution species. In addition, the successful synthesis of the heptadentate ligands through reductive amination of 2,2'-bipyridine-6-carbaldehyde with triamine ligands provides a method for the preparation of many other new 2,2'-bipyridine-appended polyamine ligands.

In summary, this research detailed in this thesis provides a sound basis for further investigations into the coordination chemistry of heptadentate ligands with small transition metal ions. The reported findings contribute to the broader understanding of coordination chemistry at the upper limits of ligand denticity.

5. References

(1) Ernst, K.; Wild, F. R.; Blacque, O.; Berke, H. Alfred Werner's Coordination Chemistry: New Insights from Old Samples. *Angew. Chem., Int. Ed.,* **2011**, *50* (46), 10780–10787.

(2) Frenking, G.; Fröhlich, N. The Nature of the Bonding in Transition-Metal Compounds. *Chem. Rev.,* **2000**, *100* (2), 717–774.

(3) Pettinari, C.; Marchetti, F.; Drozdov, A. Higher Denticity Ligands. In *Comp. Coord. Chem. II*; Elsevier Ltd., 2003; Vol. 1, pp 211–251.

(4) Hoffmann, R.; Alvarez, S.; Mealli, C.; Falceto, A.; Cahill III, T. J.; Zeng, T.; Manca, G. From Widely Accepted Concepts in Coordination Chemistry to Inverted Ligand Fields. *Chem. Rev.,* **2016**, *116* (14), 8173–8192.

(5) Power, P. P. Stable Two-Coordinate, Open-Shell (d^1–d^9) Transition Metal Complexes. *Chem. Rev.,* **2012**, *112* (6), 3482–3507.

(6) Eisenhart, R. J.; Clouston, L. J.; Lu, C. C. Configuring Bonds between First-Row Transition Metals. *Acc. Chem. Res.,* **2015**, *48* (11), 2885–2894.

(7) Davis, T. L.; Watts, J. L.; Brown, K. J.; Hewage, J. S.; Treleven, A. R.; Lindeman, S. V.; Gardinier, J. R. Structural Classification of Metal Complexes with Three-Coordinate Centres. *Dalton Trans.*. **2015**, *44* (35), 15408–15412.

(8) Morris, R. H. Six Coordinate Capped Trigonal Bipyramidal Complexes. *Coord. Chem. Rev.,* **2017**, *350*, 105–116.

(9) Braunstein, P.; Danopoulos, A. A. Transition Metal Chain Complexes Supported by Soft Donor Assembling Ligands. *Chem. Rev.,* **2021**, *121* (13), 7346–7397.

(10) Sharma, S.; Dutta, S.; Dam, G. K.; Ghosh, S. K. Neutral Nitrogen Donor Ligand-based MOFs for Sensing Applications. *Chem.– Asian J.* **2021**, *16* (18), 2569–2587.

(11) Fanshawe, R. L.; Mobinikhaledi, A.; Clark, C. R.; Blackman, A. G. Overcoming the Chelate Effect: Hypodentate Coordination of Ethylenediamine, Diethylenetriamine and Tris(2-Aminoethyl)Amine in Co(III) Complexes. *Inorg. Chim. Acta* **2000**, *307*, 26–31.

(12) Childers, R. F., Jr.; Vander Zyl, K. G., Jr.; House, D. A.; Hughes, R. G.; Garner, C. S. Synthesis of a Monodentate Ethylenediamine Complex of Chromium(III) and Kinetics of Hydrolysis of Tetraaquoethylenediaminechromium(III) Cation and of Pentaaquo(2-Aminoethylammonium)Chromium(III) Cation. *Inorg. Chem.* **1968**, *7*, 749–754.

(13) Alexander, M. D.; Spillert, C. A. Monodentate Ethylenediamine Complex of Cobalt(III). *Inorg. Chem.* **1970**, *9*, 2344–2346.

(14) Lindner, E.; Trad, S.; Hoehne, Sigurd. Preparative, Spectroscopic, and Crystallographic Studies on Phosphinato Complexes of Rhenium with Bidentate Nitrogen Ligands. *Chem. Ber.* **1980**, *113*, 639–649.

(15) Blackman, A. G. Overcoming the Chelate Effect: Hypodentate Coordination of Common Multidentate Amine Ligands. *C. R. Chim.* **2005**, *8*, 107–119.

(16) House, D. A.; Steel, P. J. The First X-Ray Crystal Structures of Cobalt Complexes Containing Monodentate and Bridging Ethylenediamine Ligands. *Inorg. Chim. Acta* **1999**, *288*, 53–56.

(17) Yanovskii, A. I.; Vaskes, Kh. Kh.; Babkov, A. V.; Antipin, M. Yu.; Struchkov, Yu. T. Crystal and Molecular Structure of Cis-Dicyano(2-Amino-2'-Ammoniodiethylamine)Platinum(II) Hexacyanoplatinate(IV) $[PtDienH(CN)_2]_2[Pt(CN)_6]$. *Koord. Khim.* **1984**, *10*, 1706–1709.

(18) Mahal, G.; Van Eldik, R.; Roodt, A.; Leipoldt, J. G. The Characterization of a Ring-Opened Diethylenetriamine Complex of Platinum(II). The Crystal Structure of Pt(Dien.HCl)Cl_2. *Inorg. Chim. Acta* **1987**, *132*, 165–166.
(19) Mahal, G.; Van Eldik, R.; Roodt, A.; Leipoldt, J. G. Concerning Ring-Opened Diethylenetriamine Complexes of Platinum(II): The Crystal Structure of $[Pt(dienH)Cl_2]_2[PtCl_4].H_2O$. *Inorg. Chim. Acta* **1989**, *156*, 29–30.
(20) House, D. A.; McKee, V.; Robinson, W. T. The Crystal Structures of Chloro Mercury(II) Salts Found for Some CrN_6^{3+} Cations and Their Chromium-Nitrogen Bond-Ruptured Hydrolysis Products. *Inorg. Chim. Acta* **1989**, *157*, 15–27.
(21) Le Bris, N.; Yaouanc, J.-J.; Clement, J.-C.; Handel, H.; des Abbayes, Herve. Modes of Complexation of Linear Tri- and Tetraamines with Group 6 Metal Carbonyls. *J. Organomet. Chem.* **1995**, *487*, 131–137.
(22) Martell, A. E.; Hancock, R. D.; Motekaitis, R. J. Factors Affecting Stabilities of Chelate, Macrocyclic and Macrobicyclic Complexes in Solution. *Coord. Chem. Rev.,* **1994**, *133*, 39–65.
(23) Sato, S.; Saito, Yoshihiko. Crystal Structure of (+)589-ΛΛΛΔ-Linear Pentaethylenehexaminecobalt(III) Hexacyanocobaltate(III) Trihydrate. *Acta Crystallogr., Sect. B* **1975**, *B31*, 2456–2460.
(24) Han, J.; Liu, Y.; Tang, C.; Shen, Y.; Lu, J.; Zhang, Y.; Jia, D. Thioarsenate Anions Acting as Ligands: Solvothermal Syntheses, Crystal Structures and Characterizations of Transition Metal Complexes of Thioarsenate and Polyethyleneamine Ligands. *Inorg. Chim. Acta* **2016**, *444*, 36–42.
(25) Constable, E. C.; Housecroft, C. E. The Early Years of 2,2'-Bipyridine-a Ligand in Its Own Lifetime. *Molecules* **2019**, *24*, 3951.
(26) Kühn, F. E.; Groarke, M.; Bencze, É.; Herdtweck, E.; Prazeres, A.; Santos, A. M.; Calhorda, M. J.; Romão, C. C.; Gonçalves, I. S.; Lopes, A. D.; Pillinger, M. Octahedral Bipyridine and Bipyrimidine Dioxomolybdenum(VI) Complexes: Characterization, Application in Catalytic Epoxidation, and Density Functional Mechanistic Study. *Chem. –Eur J.* **2002**, *8* (10), 2370–2383.
(27) Scarborough, C. C.; Wieghardt, K. Electronic Structure of 2, 2′-Bipyridine Organotransition-Metal Complexes. Establishing the Ligand Oxidation Level by Density Functional Theoretical Calculations. *Inorg. Chem.,* **2011**, *50* (20), 9773–9793.
(28) Constable, E. C.; Ward, M. D.; Tocher, D. A. Spontaneous Assembly of a Double-Helical Binuclear Complex of 2,2':6',2'':6'',2''':6''',2'''':6'''',2''''':6''''',2'''''-Sexipyridine. *J. Am. Chem. Soc.* **1990**, *112*, 1256–1258.
(29) Constable, E. C.; Ward, M. D.; Tocher, D. A. Molecular Helicity in Inorganic Complexes; Bi- and Tri-Nuclear Complexes of 2,2':6',2'':6'',2''':6''',2'''':6'''',2''''':6''''',2'''''-Sexipyridine and the Crystal and Molecular Structure of Bis(μ-2,2':6',2'':6'',2''':6''',2'''':6'''',2''''':6''''',2'''''-Sexipyridine-.κ^3-N,N',N'':κ^3-N''',N'''',N''''') Dicadmium Hexafluorophosphate Acetonitrile. *J. Chem. Soc., Dalton Trans.* **1991**, 1675–1683.
(30) Baird, L. J.; Black, C. A.; Blackman, A. G. A New Series of Potentially Hexadentate Ligands Derived from 2,2'-Bipyridine. *Polyhedron* **2007**, *26*, 378–384.
(31) Hall, N. A.; Duboc, C.; Collomb, M.-N.; Deronzier, A.; Blackman, A. G. Factors Influencing Mononuclear versus Multinuclear Coordination in a Series of Potentially Hexadentate Acyclic N_6 Ligands: The Roles of Flexibility and Chelate Ring Size. *Dalton Trans.* **2011**, *40*, 12075–12082.

(32) Hall, N.; Orio, M.; Gennari, M.; Wills, C.; Molton, F.; Philouze, C.; Jameson, G. B.; Halcrow, M. A.; Blackman, A. G.; Duboc, C. Multifrequency CW-EPR and DFT Studies of an Apparent Compressed Octahedral Cu(II) Complex. *Inorg. Chem.* **2016**, *55*, 1497–1504.
(33) Constable, E. C.; Zhang, G.; Housecroft, C. E.; Zampese, J. A. Same Head, Different Scaffold: A Plethora of Structural Motifs Assembled from Silver(I) and Ditopic 2,2'-Bipyridine Ligands. *CrystEngComm* **2010**, *12*, 3724–3732.
(34) Kim, S.-D.; Kim, J.-K.; Jung, W.-S.; Chung, K.-C. Synthesis, Protonation Constants and Stability Constants for Co^{2+}, Ni^{2+}, Cu^{2+}, and Zn^{2+} Ions of 1,15-Bis(2-Pyridyl)-2,5,8,11,14-Pentaazapentadecane. *Anal. Sci. Technol.* **1996**, *9*, 411–415.
(35) Drew, M. G. B.; Nelson, J.; Nelson, S. M. Synthesis of Some Pentagonal-Bipyramidal Complexes of Manganese(II), Iron(II), Cobalt(II), Nickel(II), Copper(II), and Zinc(II) with a Heptadentate Schiff-Base Ligand and the Crystal and Molecular Structures of a Copper(II) Complex. *J. Chem. Soc., Dalton Trans.* **1981**, 1685–1690.
(36) Liao, L.-Y.; Kong, X.-R.; Duan, X.-F. Reductive Couplings of 2-Halopyridines without External Ligand: Phosphine-Free Nickel-Catalyzed Synthesis of Symmetrical and Unsymmetrical 2,2′-Bipyridines. *J. Org. Chem.* **2014**, *79* (2), 777–782.
(37) Schmalzl, K.; Summers, L. Chemical Constitution and Activity of Bipyridylium Herbicides. XII. Diquaternary Salts of 6-Methyl-2, 2'-Bipyridyl and 2-Methyl-4, 4'-Bipyridyl. *Aus. J. Chem.,* **1977**, *30* (3), 657–662.
(38) Heirtzler, F. R.; Neuburger, M.; Zehnder, M.; Constable, E. C. Preparation and Characterization of Oligo-(2, 2′-Bipyridyl) Pyrazines. *Liebigs Annalen* **1997**, *1997* (2), 297–301.
(39) Bauer, H.; Drinkard, W. A General Synthesis of Cobalt (III) Complexes; a New Intermediate, $Na_3[Co(CO_3)_3]\cdot 3H_2O$. *J. Am. Chem. Soc.,* **1960**, *82* (19), 5031–5032.
(40) *Mass Spectrometry, SCS*. https://sci-massspec.aut.ac.nz/#/MassCalculator (accessed 2026-02-13).
(41) Heider, S.; Petzold, H.; Speck, J. M.; Rüffer, T.; Schaarschmidt, D. Modification of a Hexadentate Amine Based Ligand System by N-Methylation and Effects on Spin State and Redox -Behavior of the Corresponding Transition Metal Complexes. *Z. Anorg. Allg. Chem.* **2014**, *640* (7), 1360–1367.
(42) Zhang, Y.; Qi, X.-F.; Li, C.-H.; Zhan, S.-Z. Finding a Mononuclear Cobalt(III)-Peroxo Complex with 1,4,7,10-Tetraazacyclododecane, an Intermediate for Dioxygen Reduction. *New J. Chem.* **2023**, *47* (47), 21648–21653.
(43) Bernal, I. The Phenomenon of Conglomerate Crystallization VI. Hydration Polymorphism. I. The Syntheses, Crystal and Molecular structures of $[Cis\text{-}\alpha\text{-}Co(Trien)Cl_2]Cl.nH_2O$ with n = 3,2. *J. Coord. Chem.,* **1987**, *15* (4), 337–345.
(44) Guo, X.; Li, C.; Wang, W.; Hou, Y.; Zhang, B.; Wang, X.; Zhou, Q. Polypyridyl Co Complex-Based Water Reduction Catalysts: Why Replace a Pyridine Group with Isoquinoline Rather than Quinoline? *Dalton Trans.* **2021**, *50* (6), 2042–2049.
(45) Davies, C. J.; Hilton, S. J.; Solan, G. A.; Stannard, W.; Fawcett, J. Functionalised Dien Ligands of the Type $(ArNHCH_2CH_2)_2NR$ [R=Me, $(2\text{-}C_5H_4N)CH_2$] and Their Complexes with Iron and Cobalt Halides. *Polyhedron* **2005**, *24* (15), 2017–2026.
(46) Warden, A. C.; Warren, M.; Hearn, M. T. W.; Spiccia, L. Anion Binding to Azamacrocycles: Synthesis and X-Ray Crystal Structures of Halide Adducts of $[12]aneN_4$ and $[18]aneN_6$. *New J. Chem.* **2004**, *28* (9), 1160–1167.

(47) Margulis, T. N.; Zompa, L. J. The Structure of 1,4,7,10,13,16-Hexaazacyclooctadecane (Hexacyclen) Tetra(Hydrogen Nitrate) Dihydrochloride. *Acta Cryst., Sect. B* **1981**, *37* (7), 1426–1428.
(48) Cullinane, J.; Gelb, R. I.; Margulis, T. N.; Zompa, L. J. Hexacyclen Complexes of Inorganic Anions: Bonding Forces, Structure, and Selectivity. *J. Am. Chem. Soc.* **1982**, *104* (11), 3048–3053.
(49) Job, P. Formation and Stability of Inorganic Complexes in Solution. *Ann. Chim* **1928**, *9* (10), 113–134.
(50) Mansour, F. R.; Danielson, N. D. Ligand Exchange Spectrophotometric Method for the Determination of Mole Ratio in Metal Complexes. *Microchem. J.,***2012**, *103*, 74–78.
(51) Olson, E. J.; Bühlmann, P. Getting More out of a Job Plot: Determination of Reactant to Product Stoichiometry in Cases of Displacement Reactions and n: N Complex Formation. *J. Org. Chem.,* **2011**, *76* (20), 8406–8412.
(52) Renny, J. S.; Tomasevich, L. L.; Tallmadge, E. H.; Collum, D. B. Method of Continuous Variations: Applications of Job Plots to the Study of Molecular Associations in Organometallic Chemistry. *Angew. Chem., Int. Ed.,* **2013**, *52* (46), 11998–12013.
(53) Simionato, A. V. C.; Cantú, M. D.; Carrilho, E. Characterization of Metal-Deferoxamine Complexes by Continuous Variation Method: A New Approach Using Capillary Zone Electrophoresis. *Microchem. J.,* **2006**, *82* (2), 214–219.
(54) Hill, Z. D.; MacCarthy, P. Novel Approach to Job's Method: An Undergraduate Experiment. *J. Chem. Ed.,* **1986**, *63* (2), 162.
(55) Bosque, J. M.; Almansa-López, E.; García-Campaña, A. M.; Cuadros-Rodríguez, L. Data Analysis in the Determination of Stoichiometries and Stability Constants of Complexes. *Anal. Sci.,* **2003**, *19* (10), 1431–1439.